The Plant Cell, Vol. 21: 3567–3584, November 2009, www.plantcell.org © 2009 American Society of Plant Biologists

Members of the *LBD* Family of Transcription Factors Repress Anthocyanin Synthesis and Affect Additional Nitrogen Responses in *Arabidopsis* [W][OA]

Grit Rubin,[a] Takayuki Tohge,[a] Fumio Matsuda,[b] Kazuki Saito,[b] and Wolf-Rüdiger Scheible[a,1]

[a] Max-Planck Institute for Molecular Plant Physiology, 14476 Potsdam, Germany
[b] RIKEN Plant Science Center, Tsurumi-ku, Yokohama, Kanagawa, Japan

Nitrogen (N) and nitrate (NO_3^-) per se regulate many aspects of plant metabolism, growth, and development. N/NO_3^- also suppresses parts of secondary metabolism, including anthocyanin synthesis. Molecular components for this repression are unknown. We report that three N/NO_3^--induced members of the *LATERAL ORGAN BOUNDARY DOMAIN* (*LBD*) gene family of transcription factors (*LBD37*, *LBD38*, and *LBD39*) act as negative regulators of anthocyanin biosynthesis in *Arabidopsis thaliana*. Overexpression of each of the three genes in the absence of N/NO_3^- strongly suppresses the key regulators of anthocyanin synthesis *PAP1* and *PAP2*, genes in the anthocyanin-specific part of flavonoid synthesis, as well as cyanidin- but not quercetin- or kaempferol-glycoside production. Conversely, *lbd37*, *lbd38*, or *lbd39* mutants accumulate anthocyanins when grown in N/NO_3^--sufficient conditions and show constitutive expression of anthocyanin biosynthetic genes. The *LBD* genes also repress many other known N-responsive genes, including key genes required for NO_3^- uptake and assimilation, resulting in altered NO_3^- content, nitrate reductase activity/activation, protein, amino acid, and starch levels, and N-related growth phenotypes. The results identify *LBD37* and its two close homologs as novel repressors of anthocyanin biosynthesis and N availability signals in general. They also show that, besides being developmental regulators, *LBD* genes fulfill roles in metabolic regulation.

INTRODUCTION

Nitrogen (N) and nitrate (NO_3^-) itself regulate many aspects of plant metabolism, growth, and development. These include NO_3^- uptake and assimilation (Crawford, 1995; Lejay et al., 1999), starch and organic acid metabolism (Scheible et al., 1997a), secondary metabolism (e.g., anthocyanin production) (Scheible et al., 2004; Fritz et al., 2006), germination (Alboresi et al., 2005), root architecture (Zhang et al., 1999), root and shoot development (Scheible et al., 1997b), leaf expansion (Walch-Liu et al., 2000), stomatal opening (Guo et al., 2003), flowering (Bernier et al., 1993), seed set, and senescence (Crawford, 1995; Stitt, 1999; Crawford and Forde, 2002). Some molecular components involved in regulation of these N/NO_3^- responses in *Arabidopsis thaliana* have been described. The MADS box transcription factor (TF) *ARABIDOPSIS* NITRATE REGULATED1 (ANR1) was found to act as regulator of systemic NO_3^- repression and localized NO_3^- stimulation of lateral root growth (Zhang and Forde, 1998). NITRATE TRANSPORTER1.1 (NRT1.1) was subsequently shown to act upstream of ANR1 in the signaling pathway triggering lateral root growth and root colonization of NO_3^--rich patches (Remans et al., 2006) and to regulate expression of the high-affinity NO_3^- transporter NRT2.1 (Muños et al., 2004). Also, NRT2.1 is suspected to repress lateral root initiation in response to nutritional cues by acting either as a NO_3^- sensor or signal transducer (Little et al., 2005). Recently, a CBL-interacting protein kinase, CIPK8, was shown to regulate parts of the primary NO_3^- response, including NO_3^- transporter and assimilation genes (Hu et al., 2009). Another recent report pinpoints the TF NIN-LIKE PROTEIN7 (NLP7) as an important element of NO_3^- signal transduction and regulator for N assimilation (Castaings et al., 2009). Furthermore, two bZIP TFs, ELONGATED HYPOCOTYL5 (HY5) and HY5-HOMOLOG (HYH), were suggested to be positive regulators of *NITRATE REDUCTASE2* (*NIA2*) and negative regulators of *NRT1.1* in *Arabidopsis* (Jonassen et al., 2009). Moreover, NRT1.1 was shown to regulate expression of genes involved in NO_3^- assimilation, energy metabolism, and the pentose-phosphate pathway, further supporting the view that NRT1.1 acts as a NO_3^- sensor in *Arabidopsis* (Wang et al., 2009). Despite these advances, a lot remains to be discovered about N/NO_3^- signal transduction.

Flavonoids are major secondary metabolites and widely distributed in plants. They give color to flowers and fruits (Winkel-Shirley, 2001) and are important antioxidants (Gould et al., 2002). Their antioxidant properties have nutritional value for humans and help to protect plants from oxidative damage (Nagata et al., 2003), allowing nutrient recovery in aging and senescing leaves (Hoch et al., 2003). Synthesis of flavonoids and especially anthocyanins, which are responsible for purple coloration of leaves, is stimulated by abiotic and biotic stresses (Dixon

[1] Address correspondence to scheible@mpimp-golm.mpg.de.
The author responsible for distribution of materials integral to the findings presented in this article in accordance with the policy described in the Instructions for Authors (www.plantcell.org) is: Wolf-Rüdiger Scheible (scheible@mpimp-golm.mpg.de).
[W]Online version contains Web-only data.
[OA]Open Access articles can be viewed online without a subscription.
www.plantcell.org/cgi/doi/10.1105/tpc.109.067041

and Paiva, 1995), including cold, high irradiance, excess sugar (Tsukaya et al., 1991), or limitation of inorganic macronutrients like phosphorous (P) and N (Scheible et al., 2004; Morcuende et al., 2007). There is also clear evidence that NO_3^- per se regulates secondary metabolic pathways, including parts of phenylpropanoid, flavonoid, and anthocyanin metabolism. NO_3^- addition to N-depleted *Arabidopsis* seedlings leads to a rapid repression of a set of Phe and flavonoid biosynthetic genes and decrease of Phe (Scheible et al., 2004), which are among the first recorded responses in the seedlings. These changes occur much earlier than any increase in organic N status, indicating that NO_3^- reduction is not required for these changes. Moreover, tobacco (*Nicotiana tabacum*) genotypes with low nitrate reductase (NR) activity accumulate NO_3^- but have a low organic N status comparable to the one of an N-limited wild type (Scheible et al., 1997a, 1997b, 1997c); however, unlike N-limited wild type, they display suppression of parts of secondary metabolism (Fritz et al., 2006).

In *Arabidopsis*, a number of MYB- and bHLH-type TFs are known that regulate sectors of flavonoid biosynthesis (Nesi et al., 2000, 2001; Mehrtens et al., 2005; Stracke et al., 2007; Dubos et al., 2008, Matsui et al., 2008). The *Arabidopsis* MYB TF PRODUCTION OF ANTHOCYANIN PIGMENT1 (PAP1/MYB75) is a key regulator of flavonoid/anthocyanin synthesis genes, including those encoding chalcone synthase (*CHS*), dihydroflavonol 4-reductase (*DFR*), and glutathione-S-transferase (*GST*) (Borevitz et al., 2000; Tohge et al., 2005; Wangwattana et al., 2008). The transcript levels of *PAP1* and its close homolog *PAP2*/*MYB90* are strongly induced during N or P limitation (Scheible et al., 2004; Morcuende et al., 2007) and quickly repressed after NO_3^- addition to nitrogen-depleted *Arabidopsis* seedlings (Scheible et al., 2004). The E3 ligase NITROGEN LIMITATION ADAPTATION (NLA) is an important player in a potential signaling pathway that leads to induction of anthocyanin biosynthesis during N limitation (Peng et al., 2007a, 2008). When grown in N-limiting conditions, *nla* mutants fail to induce anthocyanin biosynthetic genes (Peng et al., 2007b) and hence do not produce anthocyanins, but display early senescence. Interestingly, *nla* mutants produce normal levels of anthocyanins during P limitation or combined P and N limitation, indicating that an NLA-independent P-specific pathway exists. Players in this latter pathway might include the TFs PHOSPHATE STARVATION RESPONSE1 (Nilsson et al., 2007) and bHLH32 (Chen et al., 2007) and an interacting F-box protein (Chen et al., 2008). *PAP1* and *PAP2* were also recently described as being targets of trans-acting-small interfering RNAs derived from the *TAS4* locus (Addo-Quaye et al., 2008). Whether and how the action of trans-acting-small interfering RNAs relates to environmental stresses is unclear. Also, the signaling pathway underlying the N/NO_3^- repression is unknown.

With the advent of ATH1 GeneChips and high-throughput, quantitative real-time PCR (qRT-PCR), it became possible to obtain a near genome-wide catalog of potentially regulatory genes with N/NO_3^--dependent transcript abundances (Wang et al., 2003; Scheible et al., 2004), making them prime candidates for N regulators. Among these are three NO_3^--responsive members of the plant-specific *ASYMMETRIC LEAVES2* (*AS2*)-*LIKE* (*ASL*)/*LATERAL ORGAN BOUNDARY* (*LOB*) *DOMAIN* (*LBD*) gene family (Scheible et al., 2004) that consists of 43 members in *Arabidopsis* (Shuai et al., 2002). *ASL*/*LBD* genes encode a new family of zinc-finger DNA binding TFs, and the founder gene *LOB* was shown to recognize a 6-bp GCGGCG consensus motif and to interact with a specific bHLH protein (Husbands et al., 2007). Phylogenetic analyses subdivide the family into two classes: class I, which comprises *LOB* and *LBD1* through *LBD36*, and class II, consisting of *LBD37* through *LBD42*. Several *Arabidopsis* class I members have been implicated in plant development; *LBD6*/*AS2* functions in the specification of adaxial/abaxial organ polarity and negatively regulates expression of KNOX TFs in lateral organs (Ori et al., 2000; Semiarti et al., 2001; Byrne et al., 2002; Lin et al., 2003), *LBD36* was shown to regulate proximal-distal patterning in *Arabidopsis* petals (Chalfun-Junior et al., 2005), *LBD16* and *LBD29* are required for auxin-dependent lateral root formation (Okushima et al., 2007), *LBD18* and *LBD30* were shown to regulate tracheary element differentiation in *Arabidopsis* (Soyano et al., 2008), and *LBD30*/*JAGGED LATERAL ORGANS* is essential for *Arabidopsis* embryo development (Borghi et al., 2007). Developmental functions have also been described for a few class I *LBD* genes in maize (*Zea mays*; Bortiri et al., 2006; Evans, 2007; Taramino et al., 2007). However, no biological function was so far reported for a class II *LBD* gene.

Here, we present a reverse genetic characterization of class II *LBD37*, *LBD38*, and *LBD39* and show that LBD37 and the two homologs mediate the repressive effect of N/NO_3^- on anthocyanin biosynthesis and further affect N-responsive genes and N metabolism, thereby revealing a novel function for LBD proteins in the regulation of plant metabolism.

RESULTS

LBD37, *38*, and *39* Transcripts Are Strongly Induced by Nitrate and More Moderately by Ammonium and Gln

LBD37, *LBD38*, and *LBD39* are closely related and arose by two segmental duplications of the *Arabidopsis* genome (http://www.tigr.org/). Their transcripts increase rapidly (within minutes) and strongly (*LBD37* and *LBD38* >20-fold) after readdition of 3 mM KNO_3, but not after readdition of 3 mM KCl, to N-depleted seedlings. The transcript levels also remain 4- to 10-fold higher in seedlings grown in full nutrient conditions compared with N-deprived seedlings (see Supplemental Figure 1 online; Scheible et al., 2004). Other *LBD* gene transcripts are unaffected by N status and NO_3^- readdition (see Supplemental Figure 1 online). Rapid and strong NO_3^- induction was confirmed by qRT-PCR (Figure 1A). The response of the three *LBD* transcripts was specific for N/NO_3^-, since limitation and subsequent readdition of sugar, phosphate, or sulfate did not lead to noteworthy transcript changes (Figure 1B; see Supplemental Figure 1 online). Other important N sources, such as ammonium (NH_4^+) and Gln, also induce the three genes, although to a weaker extent (Figure 1C); for example, induction of *LBD37* 30 min after readdition of 3 mM NH_4Cl to N-limited seedlings was seven times weaker compared with 30 min readdition of NO_3^-. Induction by NH_4NO_3 was slightly higher than by KNO_3 alone, indicating that the effects of NO_3^- and NH_4^+ are somewhat additive. Glu or urea

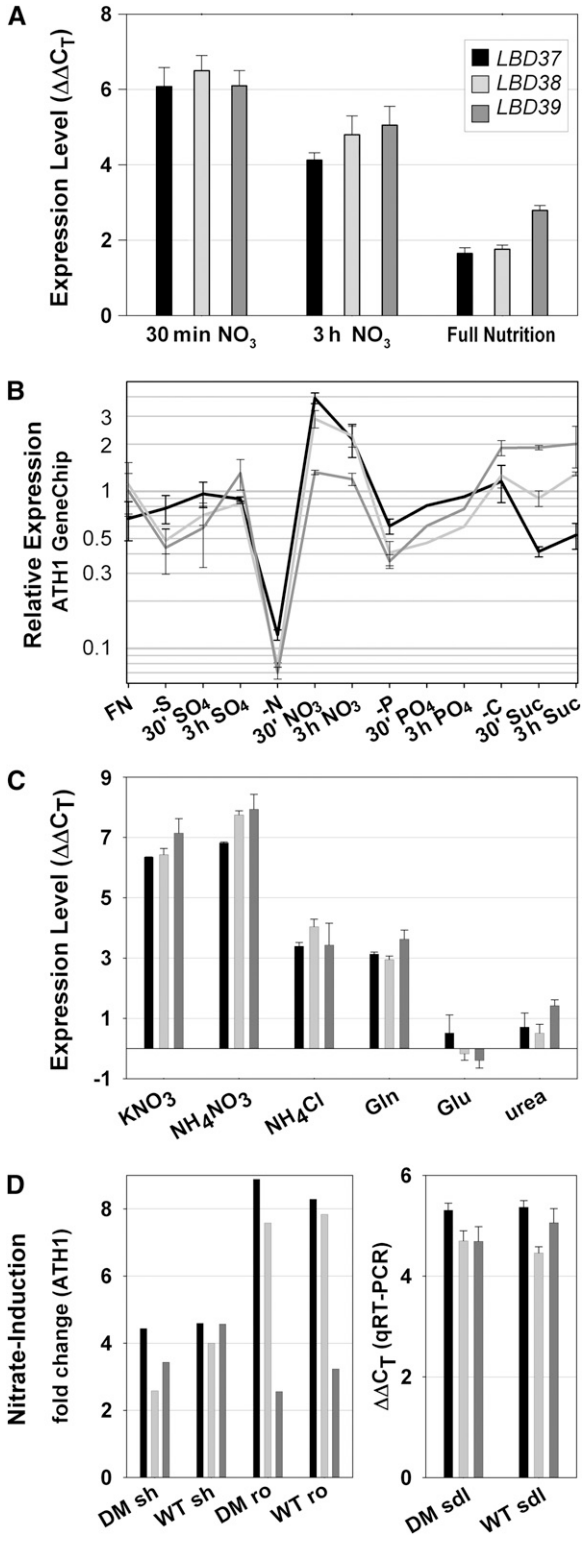

Figure 1. Nutrient-Dependent Expression of *LBD37*, *LBD38*, and *LBD39*.

(A) Relative qRT-PCR expression levels after 30 min or 3 h NO_3^- readdition to N-limited wild-type seedlings or in N-replete relative to N-limited wild-type seedlings. Data are depicted as $\Delta\Delta C_T$; i.e., a logarithmic scale; e.g., $\Delta\Delta C_T = 6$ equals a 2^6- = 64-fold induction if primer efficiency is 100% (see Supplemental Table 1 online). Gray shading is defined in the key. Results represent mean values ± SD from three independent biological replicates with two technical replicates for each.

(B) Relative expression levels derived from ATH1 GeneChip data for various nutrient stress and nutrient readdition time courses (FN, full nutrition; −S, sulfur limitation; SO_4, 3 mM potassium sulfate readdition [W.-R. Scheible and R. Morcuende, unpublished data]; −N, nitrogen limitation; NO_3, 3 mM potassium nitrate readdition [Scheible et al., 2004]; −P, phosphorous limitation; PO_4, 3 mM potassium phosphate readdition [Morcuende et al., 2007]; −C, carbon limitation; Suc, 15 mM sucrose readdition [Osuna et al., 2007]). The average expression level of each gene in all conditions was set to 1. Data represent mean values ± SD from two independent biological replicates. Gray shading is explained in **(A)**.

(C) Effect of readdition of various N sources (KNO_3, 3 mM potassium nitrate; NH_4NO_3, 1.5 mM ammonium nitrate; NH_4Cl, 3 mM ammonium chloride; Gln, 1.5 mM L-Gln; Glu, 3 mM L-Glu; 1.5 mM urea) on *LBD* transcript levels. Readditions were done for 30 min on N-limited wild-type seedlings. Results represent mean values ± SD from three independent biological replicates with two technical replicates for each. Gray shading is as in **(A)**.

(D) Nitrate induction of *LBD37*, *LBD38*, and *LBD39* in nitrate reductase-deficient *nia1 nia2* double mutants (DM). The left panel depicts public ATH1 GeneChip results from shoots (sh) and roots (ro) (Wang et al., 2004). Addition of 5 mM KNO_3 for 2 h; averaged signal ratios between nitrate-treated and chloride-treated plants are shown as reported in the supplemental data sets from Wang et al. (2004). The right panel shows qRT-PCR results (given as $\Delta\Delta C_T$) from N-starved seedlings (sdl) that were resupplied with 3 mM KNO_3 during 30 min prior to harvest. Gray shading is as in **(A)**.

had no effect on the three *LBD* transcripts (Figure 1C). The induction of the three *LBD* genes was also detectable after KNO_3 readdition to NR-deficient *Arabidopsis nia1 nia2* double mutants grown in NO_3^--free medium (ATH1 data from Wang et al. [2004] and confirmed by qRT-PCR; Figure 1D), indicating that a signal derived from NO_3^- per se already triggers the increase of the three *LBD* transcripts. Sixfold to eightfold induction of the three *LBD* transcripts was also recorded after addition of micromolar concentrations of nitrite to *Arabidopsis* roots (Wang et al., 2007).

LBD37, *LBD38*, or *LBD39* Overexpressing and Mutant Lines

Constitutive and ethanol-inducible overexpression (OX and iOX, respectively) lines were produced and homozygous T-DNA insertion mutants isolated from the SALK and Gabi-Kat collections (Alonso et al., 2003; Rosso et al., 2003). Transgenic lines were characterized for *LBD* transcript levels by RNA gel blot and qRT-PCR (Figure 2). qRT-PCR analysis revealed that the induction of *LBD* in the N-limited overexpressing lines (Figure 2B) was comparable to the strong induction in N-limited wild type after NO_3^- addition (cf. Figures 1A and 1C). By contrast, the respective *LBD* transcript was strongly reduced ($\Delta\Delta C_T = -6$ to -10) in *lbd37*, *lbd38*, and *lbd39* T-DNA insertion lines when primers downstream of the insertion site were used (Figures 2B and 2C). In the case of the *lbd37* mutant alleles (*lbd37-1* and *lbd37-2*), the insertion sites are both located in the 3′-untranslated region of the transcript (Figure 2C). Still, this led to (1) considerably reduced qRT-PCR amplification of an *LBD37* PCR product

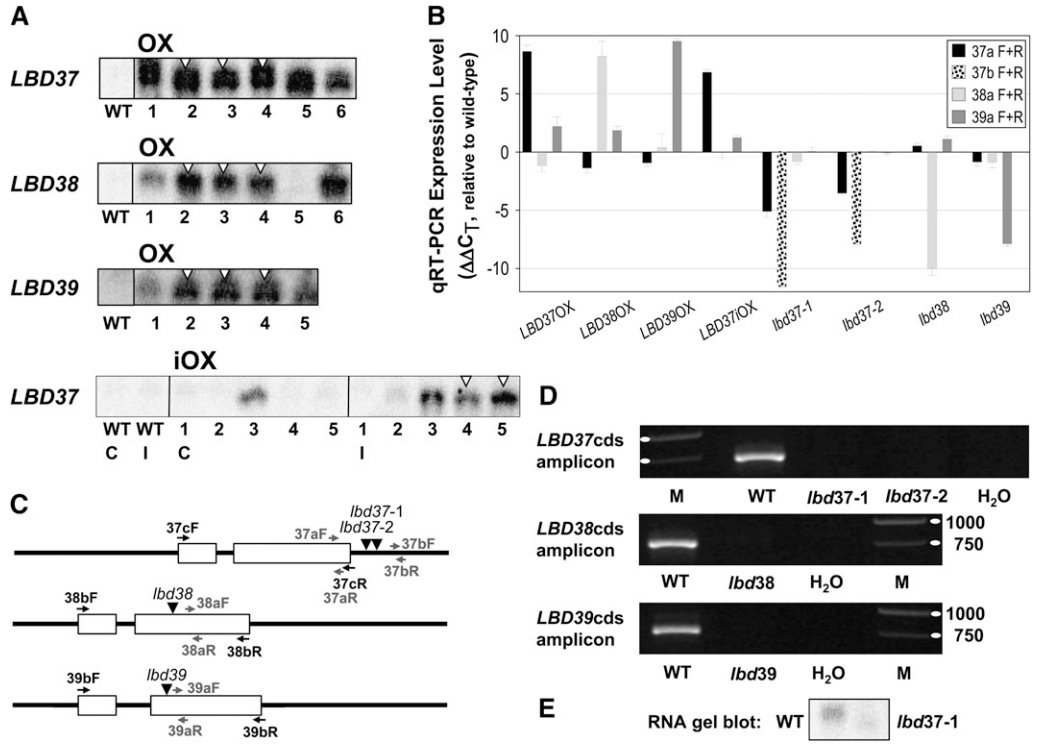

Figure 2. Molecular Characterization of *LBD* Overexpressor and T-DNA Insertion Lines.

(A) RNA gel blot analysis of *LBD* expression in five to six constitutive overexpressor lines (OX) or inducible overexpresser lines (iOX). IOX lines were tested in N-limited, noninduced control conditions (C), and after 3 h of induction (I) with 0.2% (v/v) ethanol. Note the constitutive induction in *LBD37*iOX line 3. White triangles indicate lines that were chosen for subsequent experiments.

(B) Quantitative analysis of *LBD* expression by qRT-PCR in N-limited OX and iOX lines relative to N-limited wild type and in previously N-starved T-DNA insertion lines after 30 min resupply of 3 mM KNO_3 relative to equally treated wild type. Note the logarithmic nature of the *y* axis (cf. legend to Figure 1A). Primers used are depicted in **(C)** and are given in Supplemental Table 1 online. Results represent mean values ± SD from three biological replicates/independent lines with two technical replicates for each.

(C) Graphical depiction of *LBD* gene structures, T-DNA insertion sites, and primer annealing sites. White boxes indicate exons and black lines untranslated regions or introns. T-DNA insertions are represented by black triangles and primers by arrows. Primers shown in gray were used for the analysis presented in **(B)**, whereas those shown in black were used for the analysis shown in **(D)**.

(D) Amplification of PCR products comprising the entire *LBD* gene coding sequence (LBDcds) from cDNA samples of wild-type and *lbd* T-DNA insertion mutants. N-starved seedlings were supplied with 3 mM KNO_3 for 30 min prior to harvest. Amplification was performed for 25 cycles. A negative control (water) and a DNA marker (M) are shown for comparison. The 1000- and 750-bp marker DNA bands are indicated by white ellipses. Each LBDcds amplicon is expected to be ~750 bp long. cDNA preparations used were of comparable concentrations as determined by qRT-PCR ($C_{T\ UBQ10}$ = 16.7 to 17.1; Czechowski et al., 2005). Representative results for each PCR amplification are shown.

(E) RNA gel blot analysis of *LBD37* expression in the wild type and *lbd37*-1 mutant after 30 min nitrate readdition to previously N-starved seedlings. The signal in the wild type corresponds to a size of 1.05 to 1.1 kb being very similar to the sizes of *LBD37* full-length RNAs deposited in GenBank (e.g., BX830145 or AF447894). The signal in *lbd37*-1 is much weaker and of aberrant size.

upstream of the insertion sites (Figure 2B), (2) strongly reduced amplification of another *LBD37* PCR product downstream of the insertion sites, (3) no detectable amplification of RT-PCR products spanning the entire *LBD37* coding sequence (Figure 2D), and (4) an aberrant and reduced RNA gel blot signal for *LBD37* (Figure 2E). We conclude that all analyzed *lbd* mutants are strong reduction-of-function or null alleles.

Altered Anthocyanin Pigmentation in LBD37, LBD38, or LBD39 Overexpressers and Mutants

OX lines were investigated in N-limited conditions when the three *LBD* genes display very low expression (Figure 1B). When grown on agar plates or in liquid cultures (Scheible et al., 2004), wild-type seedlings turn reddish within 2 d after the N source (i.e., NO_3^-) is removed (Figure 3A), due to accumulation of anthocyanins. By contrast, the OX lines of each of the three *LBD* genes remained green (Figure 3B; see Supplemental Figure 2A online). Homozygous T-DNA insertion mutants for the three *LBD* genes were grown with sufficient N/NO_3^-, conditions in which the genes show high expression in the wild type. The *lbd37*, *lbd38*, and *lbd39* mutants accumulated anthocyanin in the leaves (Figures 3C and 3D; see Supplemental Figure 2B online), whereas the wild type did not (Figure 3E). The suppression of anthocyanin synthesis in *LBD37*, *LBD38*, or *LBD39* OX lines was

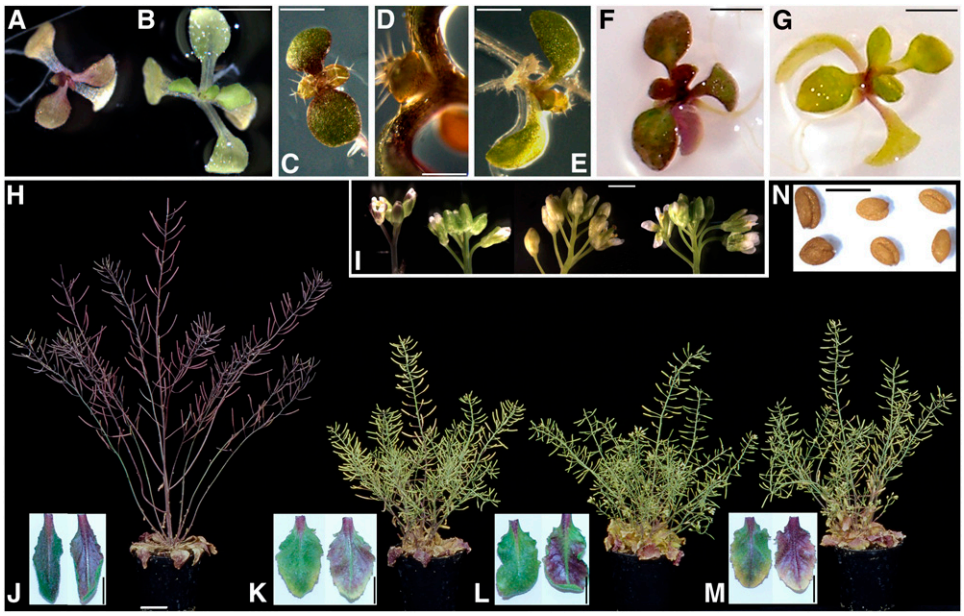

Figure 3. Anthocyanin Pigmentation Phenotypes.

(A) and **(B)** Nine-day-old N-limited wild-type **(A)** and N-limited *LBD37* OX seedlings **(B)**. For additional photographs, see Supplemental Figure 2 online.
(C) to **(E)** Nine-day-old nitrate-replete *lbd37-1* T-DNA mutant seedlings (**[C]** and **[D]**) and a NO_3^--replete wild-type seedling **(E)**. For additional photomicrographs, see Supplemental Figure 2 online.
(F) and **(G)** Nine-day-old wild-type seedling **(F)** and a *LBD37* overexpresser seedling **(G)** grown in medium containing 6% sucrose.
(H) Adult wild-type, *LBD37*, *LBD38*, and *LBD39* OX plants (from left to right) grown in high illumination (600 μE).
(I) Flowers of wild-type, *LBD37*, *LBD38*, and *LBD39* OX plants (from left to right) grown in –N soil.
(J) to **(M)** Adaxial (left) and abaxial (right) surface of mature rosette leaves from wild-type **(J)**, *LBD37* **(K)**, *LBD38* **(L)**, and *LBD39* **(M)** OX plants grown in –N soil.
(N) Seeds of wild-type, *LBD37*, and *LBD38* OX plants (from left to right, two seeds each) from plants as shown in **(H)**.
Bars = 4 mm in **(A)**, **(B)**, **(F)**, **(G)**, and **(I)**, 2 mm in **(C)** and **(E)**, 0.4 mm in **(D)**, 2 cm in **(H)**, 1 cm in **(J)** to **(M)**, and 0.5 mm in **(N)**.

robust. Other stress conditions (e.g., cold, high concentrations of sugar, and P limitation) that stimulate anthocyanin production were unable to override the effect of *LBD* OX in seedlings (Figures 3F and 3G; see Supplemental Figure 2C online).

The pigmentation phenotype of the OX lines was present throughout development. When grown in N-limiting conditions or under high irradiance (Figure 3H), the wild type accumulated anthocyanins in leaves, stems, flowers, and siliques, but the OX plants did not. However, some anthocyanin was noticeable in mature and senescing leaves of the OX plants (Figure 3H). Mature OX leaves had anthocyanin on the lower (abaxial) leaf surface and in the leaf petiole, but not the upper (adaxial) leaf surface (Figures 3J to 3M). This indicates that LBD37, LBD38, or LBD39 lose their strong negative effect in leaves with increasing age. Consistent with this observation, transcript levels of the three genes drop sharply with age in wild-type rosette leaves (data from AtGenExpress; Schmid et al., 2005). *LBD* OX seeds also gave rise to a slight transparent testa phenotype (Figure 3N), indicating reduced proanthocyanin and condensed tannin synthesis in the *Arabidopsis* seed coat. Consistently, the three genes are not expressed in wild-type seeds (data from AtGenExpress; Schmid et al., 2005). In addition to their striking pigmentation phenotypes, the soil-grown mature *LBD* OX plants displayed a reduction in shoot growth during reproductive stages (Figure 3H, cf. ultimate Results section).

LBD37 Localizes to the Nucleus

LBD genes are thought to encode zinc-finger TFs. Some class I family members have previously been shown to localize to the nucleus (Husbands et al., 2007; Okushima et al., 2007). The subcellular localization for class II LBDs has not yet been confirmed. We created a fusion of LBD37 to the C terminus of green fluorescent protein (GFP) expressed under control of the cauliflower mosaic virus 35S promoter (P35S). The *P35S:GFP-LBD37* construct was transformed into wild-type plants, and transgenic lines with high GFP fluorescence were selected. When grown in N-limiting conditions, the GFP-expressing transgenic lines failed to produce anthocyanin (see Supplemental Figures 3A and 3B online), as did constitutive *LBD37* OX plants. Thus, the GFP-LBD37 fusion protein is functional. GFP fluorescence was then examined in the leaves of seedlings and found to localize to nuclei of *P35S:GFP-LBD37* plants (see Supplemental Figures 3C to 3G online). These results indicate that GFP-LBD37 fusion protein was targeted to the nucleus, consistent with its predicted role as TF.

Flavonoid Profiling Reveals Specific Changes of Cyanidin Glycosides in *lbd* Mutants and *LBD* OX Lines

To analyze whether the LBDs affect flavonoid metabolism in general or only in specific sectors, we next analyzed the flavonoid metabolite profiles in shoot material of (1) 9-d-old N-limited *LBD37* OX, *LBD38* OX, and wild-type seedlings and (2) 9-d-old N-replete *lbd37*, *lbd38*, *lbd39*, and *lbd38 lbd39* mutants and wild-type seedlings (Figure 4; see Supplemental Figure 4 online). Compared with N-limited wild types, independent N-limited *LBD37* or *LBD38* OX lines showed an 80 to 90% lower content of two cyanidin derivatives (Figures 4A and 4B), for example, cyanidin 3-*O*-[2-*O*-(2-*O*-(sinapoyl) xylosyl) 6-*O*-(*p*-*O*-coumaroyl) glucoside] 5-*O*-[6-*O*-(malonyl) glucoside] (*m/z* = 1343; A11; Tohge et al., 2005) and cyanidin 3-*O*-[2-*O*-(6-*O*-(sinapoyl) xylosyl) 6-*O*-(p-*O*-(glucosyl)-*p*-coumaroyl) glucoside] 5-*O*-(6-*O*-malonyl) glucoside (*m/z* = 1181; A9; Tohge et al., 2005). The former is the most abundant and major anthocyanin species that accumulates in *PAP1* OX plants (Tohge et al., 2005). The levels of these cyanidin derivatives in N-limited *LBD37* or *LBD38* OX lines were as low as in NO_3^--replete wild type (Figures 4A and 4B; see Supplemental Figure 4 online), indicating that *LBD* OX fully phenocopies the reduction of these two metabolites that occurs in NO_3^--fed wild-type seedlings. By contrast, the two *lbd37* T-DNA mutants showed an approximately sixfold increased level of these cyanidin glycosides in comparison to the wild type when grown in NO_3^--sufficient conditions (Figures 4A and 4B). Similarly, cyanidin glycoside A9 and A11 levels were also increased in *lbd38* and *lbd39* mutants, and the effect was even slightly more pronounced in an *lbd38 lbd39* double mutant. Other cyanidin derivatives were not reliably detected in the samples.

Flavonol glycosides (named F1 to F6 according to Tohge et al., 2005) derived from quercetin or kaempferol were largely unchanged in the OX or mutant seedlings irrespective of NO_3^- supply (Figures 4C to 4G; see Supplemental Figure 4 online). The OX and mutant lines also produce normal levels of lignins as detected by phloroglucinol staining of stem sections (see Supplemental Figure 4H online). Together these results suggest (1) a specific effect of the LBDs on anthocyanin metabolism downstream of dihydroquercetin and (2) that *LBD37* or *LBD38* OX mimics the effect of N/NO_3^- supply on cyanidin glycoside levels.

LBD OX Phenocopies the Transcriptional Changes Found in the Cyanidin Pathway after NO_3^- Addition to N-Limited Wild-Type Seedlings and Results in a Mirror Image of the Changes Observed in *PAP1* Overexpressers

N/NO_3^- deficiency or *PAP1* OX strongly induce a shared set of genes involved in late flavonoid synthesis in *Arabidopsis* (Lillo et al., 2008). N/NO_3^- deficiency also leads to strong transcriptional induction of *PAP1* and *PAP2* (Scheible et al., 2004). To further test and cement the emerging role of the *LBD* genes in N/NO_3^--dependent repression of anthocyanin biosynthesis, we used qRT-PCR to analyze the expression of structural or regulatory genes known to be involved in early or late steps of flavonoid biosynthesis. Expression was compared in (1) N-limited *LBD* OX seedlings versus N-limited wild-type seedlings, (2) NO_3^--fed (i.e., N-replete) versus N-limited wild-type seedlings, (3) NO_3^--fed *pap-1D* seedlings (Borevitz et al., 2000) versus NO_3^--fed wild-type seedlings, and (4) NO_3^--fed *lbd37*, *lbd38*, and *lbd39* mutant seedlings versus NO_3^--fed wild-type seedlings (Figure 5; see Supplemental Figures 5 to 7 online).

The analyses revealed that independent *LBD37* OX or *LBD38* OX lines had decreased expression of *PAP1* and *PAP2*, resembling the decrease found in NO_3^--fed wild-type seedlings or in wild-type seedlings after short-term NO_3^- readdition (Scheible et al., 2004) (Figure 5). Extension of the comparison to flavonoid biosynthetic genes showed that (1) *LBD37* or *38* OX strongly (often 5- to 10-fold) represses late genes encoding pathway steps downstream of dihydroquercetin, such as cyanidin biosynthesis (i.e., *DFR*, *ANTHOCYANIDIN SYNTHASE*, *ANTHOCYANIN GLYCOSYLTRANSFERASE*, *ANTHOCYANIN ACYLTRANSFERASE*, and *GST*), including also a gene (*GLUT8*) encoding a putative carbohydrate transmembrane transporter upregulated by PAP1 that might be involved in vacuolar transport of cyanidin glycosides (Tohge et al., 2005; cf. Figures 5 and 6). Moreover, analysis of the same set of genes in *lbd37*, *lbd38*, and *lbd39* mutants revealed that the genes downregulated in the OX lines remain induced in NO_3^--replete *lbd37 lbd38* and *lbd39* mutants (see Supplemental Figure 5 online), which is consistent with the observed anthocyanin accumulation (Figures 3C and 3D; see Supplemental Figure 2B online).

Genes encoding steps in phenylpropanoid metabolism (e.g., *PHENYLALANINE AMMONIUM LYASE* [*PAL*], *CINNAMATE-4-HYDROXYLASE*, or *4-COUMARATE:COA LIGASE*) or early steps in flavonoid synthesis (*CHS*, *CHALCONE ISOMERASE* [*CHI*], or *FLAVANONE 3-HYDROXYLASE* [*F3H*]), as well as genes encoding flavonol glycosyltransferases not specific for anthocyanins or steps in proanthocyanin biosynthesis (e.g., *BANYULS*), were not or only very weakly (less than twofold) affected by *LBD* OX (see Supplemental Figure 6A online), showing that *LBD* OX in seedlings specifically represses anthocyanin synthetic genes. N/NO_3^- also did not affect these genes much; *PAL3* and *UDP-GLUCOSYL TRANSFERASE 78D1* (*UGT78D1*) were approximately twofold induced, and *CHS*, *FLAVONOID 3′ HYDROXYLASE* (*F3′H*), and *UGT71C1* were approximately twofold to threefold repressed in the comparison of N/NO_3^--fed versus N-limited wild types. The same was also observed for *PAP1* OX seedlings: *PAL* genes, *CHS*, *CHI*, and *F3H* were largely unaffected; only *F3′H* and *UGT78D2* showed a slight/moderate induction (see Supplemental Figure 6A online). These results with seedlings are in slight contrast with previous studies with leaves of rosette stage *pap1-D* plants (Borevitz et al., 2000; Tohge et al., 2005), where some phenylpropanoid metabolism genes and early genes in flavonoid biosynthesis were moderately induced.

Besides *PAP1* and *PAP2*, we analyzed the expression of additional regulatory genes involved in the regulation of anthocyanin, procyanidin, flavonoid, or phenylpropanoid biosynthesis, including several *MYB* family TF genes (*MYB3*, *MYB4*, *MYB11*, *MYB12*, *MYB32*, *MYB66/WEREWOLF*, *MYB111*, *MYB123/TRANSPARENT TESTA2* [*TT2*], *MYB0/GLABRA1* [*GL1*]), bHLH family TF genes (*GL3*, *ENHANCER OF GLABRA1* [*EGL1*], and *TT8*), WD40 protein (*TRANSPARENT TESTA GLABRA1* [*TTG1*]), and others (*TRANSPARENT TESTA1*, *HY5*, *HYH*, *ANTHOCYANINLESS2*, and *TTG2*) (Figure 5C; see Supplemental Figure 6B online). The analysis showed that three TF genes had an appreciably changed

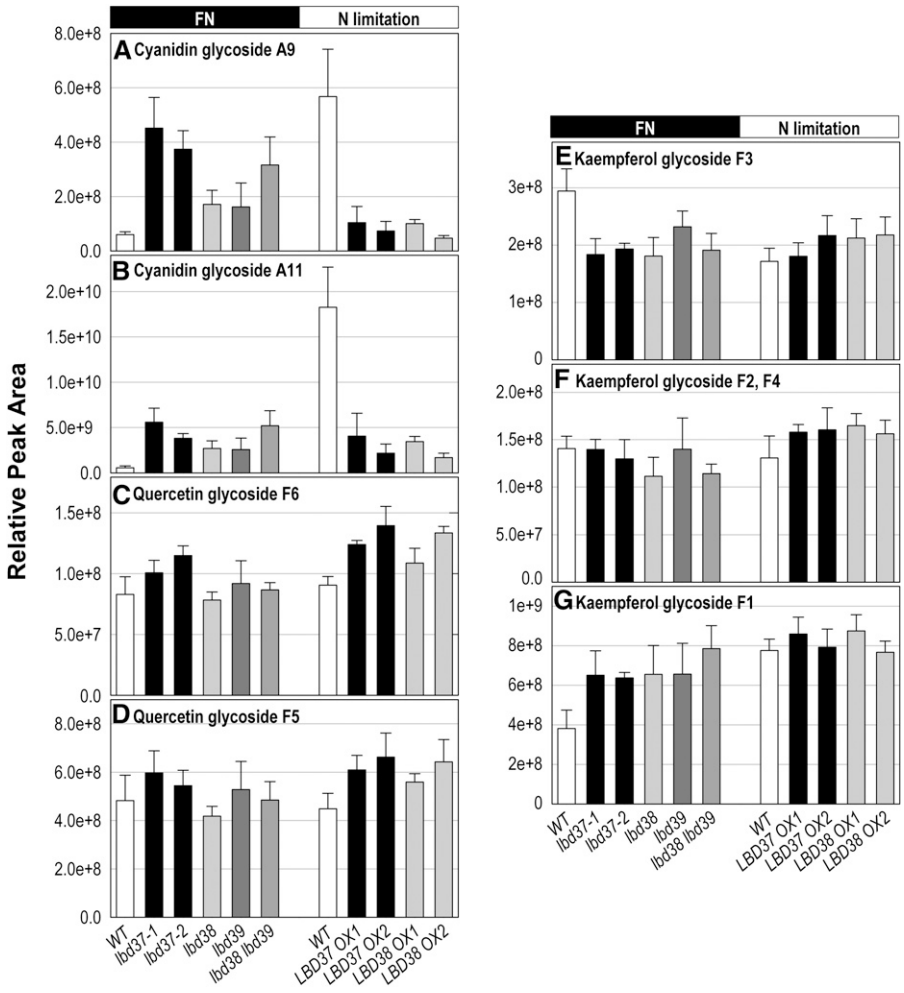

Figure 4. Targeted Flavonoid Profiling.

Contents of seven detected cyanidin and flavonol glycoside species in shoot material from NO_3^--fed (FN, black horizontal bar) and N-limited (N limitation, white horizontal bar) wild type, *lbd* mutant lines, two independent *LBD37* OX, and two *LBD38* OX lines. Results are mean values ± SD from three biological replicates for each genotype. Cyanidin derivatives and flavonol glycosides are named according to Tohge et al. (2005).

(A) Cyanidin 3-*O*-[2"-*O*-(2"'-*O*-(sinapoyl) xylosyl) 6"-*O*-(*p*-*O*-coumaroyl) glucoside] 5-*O*-[6""-*O*-(malonyl) glucoside], A9 (*m/z* = 1181).

(B) Cyanidin 3-*O*-[2"-*O*-(6"'-*O*-(sinapoyl) xylosyl) 6"-*O*-(*p*-*O*-(glucosyl)-p-coumaroyl) glucoside] 5-*O*-(6""-*O*-malonyl) glucoside, A11 (*m/z* = 1343).

(C) Quercetin 3-*O*-[2"-*O*-(rhamnosyl) glucoside] 7-*O*-rhamnoside, F6 (*m/z* = 757).

(D) Quercetin 3-*O*-glucoside 7-*O*-rhamnoside, F5 (*m/z* = 611).

(E) Kaempferol 3-*O*-[2"-*O*-(rhamnosyl) glucoside] 7-*O*-rhamnoside, F3 (*m/z* = 741).

(F) Kaempferol 3-*O*-glucoside 7-*O*-rhamnoside or quercetin 3-*O*-rhamnoside 7-*O*-rhamnoside, F2 or F4 (*m/z* = 595).

(G) Kaempferol 3-*O*-rhamnoside 7-*O*-rhamnoside, F1 (*m/z* = 579).

transcript level in *LBD* OX; *TT1* was strongly induced, while *MYB11* and *TT8* were threefold to fourfold repressed (Figure 5C). *PAP1* OX again resulted in a phenotype opposite to that of *LBD37/38* OX with respect to *TT8* and *TT1*. N/NO_3^- had a wider effect; in addition to a strong inductive effect on *TT1*, it also led to a clear induction of *MYB111*, *EGL1*, and *GL1* and a repression of *MYB123/TT2* (see Supplemental Figure 6B online). The effects on *MYB11* and *TT8* transcript levels were weak (Figure 5C).

The set of anthocyanin synthesis genes repressed in constitutive *LBD* OX lines was subsequently also analyzed in inducible *LBD37* OX (iOX) lines (see Supplemental Figure 7 online; Figure 2). The results showed that iOX leads to the same general changes as observed before in the constitutive OX lines, except that the decrease of the *PAP1*, *PAP2*, and anthocyanin pathway transcripts found after 3 or 6 h induction was less pronounced. Possibly, the endogenous *PAP1* and *PAP2* transcripts and PAP1 and PAP2 proteins were stable enough to prevent a more dramatic decrease. The result indicates that the changes detected in constitutive OX lines are specific and not merely an unrelated phenotype.

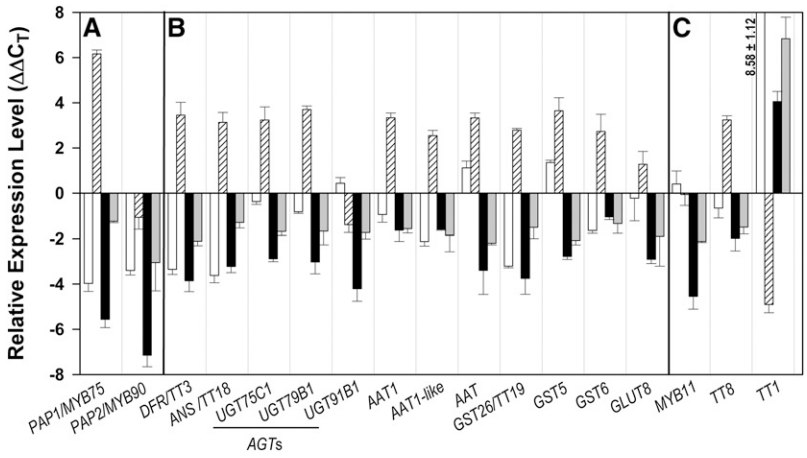

Figure 5. Expression Levels of Structural and Regulatory Anthocyanin Synthesis Genes.

(A) Regulatory genes *PAP1* and *PAP2*.
(B) Anthocyanin synthesis genes.
(C) Regulatory genes *MYB11*, *TT8*, and *TT1*.
Shown are relative expression changes in NO_3^--fed versus N-limited wild types (white bars), in the NO_3^--fed *pap1-D* activation tagging line versus NO_3^--fed wild-types (hatched bars), and in N-limited *LBD37* and *LBD38* OXs versus N-limited wild-types (black and gray bars, respectively). Results represent mean values ± SD from three independent biological replicates/lines with two technical replicates for each. Shown are genes with $|\Delta\Delta C_T| \geq 1.5$ in *LBD37* or *38* OX lines. Note the logarithmic character of the *y* axis (cf. legend to Figure 1A).

In summary, transcript changes found in *LBD37/38* OX lines and in the *PAP1* OX line reveal a broad overlap and also surprisingly well reflect the changes found in the comparison of N/NO_3^--fed and N-limited wild-type seedlings (Figures 5 and 6). Together, the results pinpoint the *LBD37* TF and its close homologs as novel molecular components involved in the transmission of an N/NO_3^--derived signal that suppresses anthocyanin synthesis via repression of *PAP1* and *PAP2*.

Transcriptome Profiling Reveals a More Profound Role of the LBDs in N Signaling

The analysis presented so far was focused on flavonoid/anthocyanin biosynthesis. To test whether *LBD37*, *38*, and *39* have only this specific function or whether they may have a more widespread role in NO_3^-/N regulation, we investigated the global transcript profiles of N-limited *LBD37* and *LBD38* OX lines, as well as N-limited and N/NO_3^--replete wild-type seedlings with Affymetrix ATH1 GeneChips. N/NO_3^- availability in the wild type led to a ≥3-fold change of 783 gene transcripts (Figure 7; see Supplemental Data Set 1 online), resembling results of earlier studies (Wang et al., 2003; Scheible et al., 2004; 581 of these transcripts were also ≥2-fold changed in the former study). Interestingly, *LBD37* or *LBD38* OX led to a ≥3-fold repression of 100 or 76 gene transcripts, respectively, while only very few gene transcripts were induced (Figure 7), revealing that the LBDs mainly function as transcriptional repressors, as noted before. Remarkably, 63 to 71% of the gene transcripts that were ≥3-fold repressed in *LBD37* or *LBD38* OX seedlings were also ≥3-fold repressed by N/NO_3^- availability in wild-type seedlings, suggesting that the LBDs play a role in the regulation of transcriptional N responses. This percentage even rises to 69 to 80% when gene transcripts with ≥2-fold repression are considered (see Supplemental Data Set 1 online).

Among the N/NO_3^--repressed genes with reduced transcript levels in *LBD37* or *LBD38* OX seedlings were *PAP1* and *PAP2*, several genes encoding glutaredoxin, senescence-associated genes, or the nitrate transporter gene *NRT2.5* (see Supplemental Figures 8A and 8B and Supplemental Data Set 1 online). Besides, several additional gene transcripts involved in NO_3^- uptake and assimilation were altered in *LBD* OX, including *NIA1*, which encodes NR (see Supplemental Figure 8C online) and to some lesser extent also *NIA2*, the NO_3^- transporter genes *NRT1.1*, *NRT2.1*, *NRT2.2*, and *NRT3.1*, as well as the Gln synthetase gene *GLN1.4* (see Supplemental Figures 8C, 8G, and 8H online). In addition, a number of N-responsive gene transcripts encoding regulatory components were altered in *LBD* OXs. These include TFs (WRKY38, NF-YA10, and NAC55) and several (receptor) protein kinases or the Glu-receptor protein GLR1.2 (see Supplemental Figures 8A, 8B, and 8I online). Closer inspection of the ATH1 GeneChip results also confirmed the repression of anthocyanin synthetic genes (see Supplemental Figure 8J online) in *LBD* OX seedlings, although the individual transcript responses were generally less pronounced than observed with qRT-PCR (Figure 5).

We also compared *lbd37* and *lbd38* seedlings grown in NO_3^--replete conditions with NO_3^--replete wild-type seedlings. There were only very few (≥3-fold) changes (1 or 12 transcripts induced in *lbd37* or *lbd38*, respectively; no genes ≥3-fold repressed in both mutants) with the most noteworthy being the 3.3-fold induction of *NRT2.1* in *lbd38* (see Supplemental Data Set 2 online).

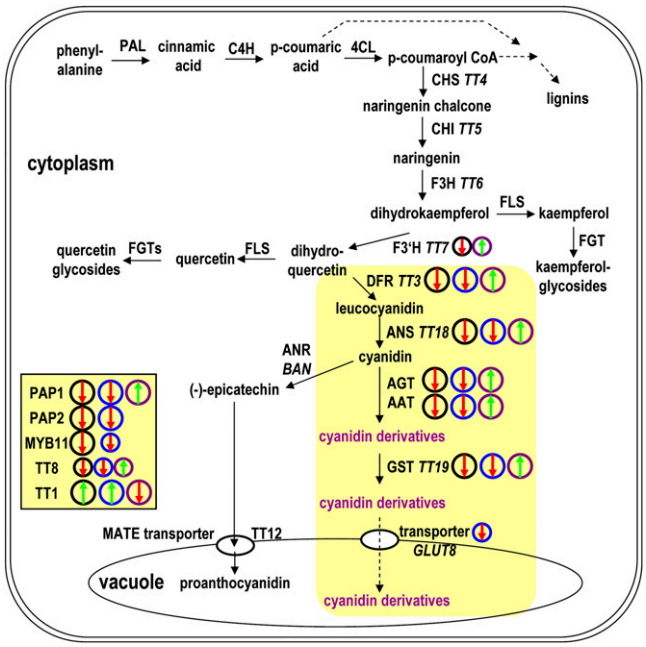

Figure 6. Summary of the Effects of Nitrate, *LBD37*, *38*, or *39*, and *PAP1* Overexpression on the Anthocyanin Biosynthesis Pathway.

Anthocyanin-specific pathway steps in flavonoid metabolism are shown in a yellow background. Regulatory genes that were found to be considerably misexpressed in *LBD* OXs are shown in the yellow shaded box to the left. Black, blue, and purple circles mark the pathway steps/genes affected by NO_3^-, *LBD37* OX, or *PAP1* OX, respectively. Red arrows indicate repression and green arrows induction. The size of the circles gives an indication of the strength of the changes. Contents of cyanidin derivatives are low in N/NO_3^--fed wild-type plants and N-limited *LBD37*, *LBD38*, and *LBD39* OX lines and accumulate in N/NO_3^--fed *lbd37*, *lbd38*, and *lbd39* mutants and *PAP1*OXs (Borevitz et al., 2000; Tohge et al., 2005). Major quercetin- and kaempferol-glycosides were unchanged. PAL, phenylalanine ammonium lyase; C4H, cinnamate-4-hydroxylase; 4CL, 4-coumarate:CoA ligase; CHI, chalcone isomerase; FLS, flavonol synthase; FGT, flavonol glycosyltransferase; BAN, anthocyanidin reductase BANYULS; ANS, anthocyanidin synthase; AGT, anthocyanin glycosyltransferase; AAT, anthocyanin acyltransferase. Pathways are depicted according to Tohge et al. (2005).

LBD37, 38, and 39 Repress Genes Involved in NO_3^- Uptake/Assimilation

We aimed to confirm the results observed for genes involved in NO_3^- uptake and reduction (see Supplemental Figure 8H online), including NR genes *NIA1*, *NIA2*, NO_3^- transporter genes *NRT1.1*, *NRT2.1*, *NRT2.1*, and *NRT2.5*, as well as *GLN1.4* and *G6PD2*, the latter being involved in the provision of carbon skeletons required for N assimilation. Expression analysis by qRT-PCR confirmed that *NRT2.1*, *NRT2.2*, *NIA1*, and *G6PD2* are induced 3 h (and already 30 min) after readdition of NO_3^- to N-limited wild type (Figure 8; see Supplemental Figure 9 online; Scheible et al., 2004). This induction is abolished or reversed in N-replete wild types, which is attributable to organic nitrogen compounds like Gln (Krapp et al., 1998; Lejay et al., 1999; Nazoa et al., 2003). By contrast, *NRT2.5* and *GLN1.4* are repressed 3 h (but not 30 min) after NO_3^- readdition (Scheible et al., 2004; Figure 8), suggesting repression is linked to NO_3^- reduction. Consequently and similar to *NIA1*, these two genes are repressed after Gln readdition to N-starved wild type ($\Delta\Delta C_T$ = −6.91, −1.82, and −2.25 for *NIA1*, *NRT2.5*, and *GLN1.4*, respectively, after 3 h).

qRT-PCR analysis further confirmed that expression of *NIA* genes was 3- to 6-fold reduced, and expression of *NRT1.1*, *NRT2.1*, *NRT2.2*, and *NRT2.5* was 2- to 10-fold lower in the OX lines compared with the wild type (Figure 8; cf. Supplemental Figure 8H online). In addition, expression of *GLN1.4* and *G6PD2* was significantly decreased in the OX lines. These results are further corroborated by similar changes in *LBD37* iOX lines and reciprocal, yet weaker changes in *lbd37*, *lbd38*, and *lbd39* mutants (Figure 8; see Supplemental Figure 9A online) and suggest that LBD37/38/39 expression mimics the effect of organic N compounds on expression of *NIA1*, *NIA2*, *NRT2.1*, *NRT2.5*, or *GLN1.4.*

LBD37, 38, and 39 Affect N Status, Growth, and N-Dependent Shoot Branching

Reduced expression of genes required for NO_3^- uptake and reduction caused by mimicry of N availability in LBD OX lines should eventually lead to symptoms of N limitation, reduced plant N status, and ultimately growth. The smaller stature of mature LBD OX plants (Figures 3H and 9A) is in agreement with this. To further test the hypothesis, we performed a biochemical analysis of mature wild-type and LBD OX lines (Figures 9B to 9F). This revealed that LBD OX lines contain 40 to 65% less NO_3^- (Figure 9B) and have 100 to 150% higher starch levels (Figure 9C) than wild-type plants. Moreover, the OX lines displayed a 35 to 60% reduction in maximal NR activity, while NR activation increased from ~60% in the wild type to 90 to 100% in OX lines (Figure 9D). Furthermore, protein content was decreased by up to 20% (Figure 9E), and total amino acid content dropped in the OX lines. This was mostly due to a fourfold to fivefold decrease of Gln but was also due to substantial decreases in other amino acids, such as Asp, Asn, Arg, or Gly (Figure 9F). The strong decrease of Gln and Asn in the OX lines is further confirmed by a reciprocal increase of Gln and Asn in *lbd* mutants (see Supplemental Figure 10 online). The analyzed molecular, physiological, and biochemical parameters all show that *LBD37*, *38*, or *39* have more widespread effects and negatively affect N assimilation and, as a consequence, plant N status and growth. Besides, *LBD37*, *38*, or *39* OX also alters N-dependent basal shoot branching (see Supplemental Figure 11 online). *Arabidopsis* wild-type plants produce no basal rosette branches when grown in N-limited conditions. In comparison, *LBD* OX plants grow as many basal shoot branches in N-limited conditions as they do or the wild type does in N-replete conditions. This result is again consistent with the idea that these LBD proteins represent important molecular components to signal N/NO_3^- availability.

DISCUSSION

Nitrogen and NO_3^- (as the major form of N available to many plants) are macronutrients and signals for plant growth and metabolism, but still little is known about the molecular

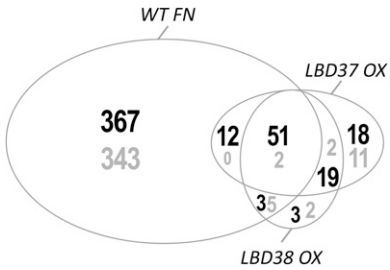

Figure 7. Shared Transcriptional Changes in Response to Nitrogen Status and *LBD37* or *LBD38* Overexpression.

The Venn diagram indicates the number of gene transcripts that are ≥3-fold decreased (black numbers) or increased (gray numbers) in either N-limited *LBD37* or *LBD38* overexpressing seedlings or N-replete wild-type (WT FN) seedlings in comparison to N-limited wild-type seedlings. Data were calculated from the average of three biological replicates for each condition (see Supplemental Data Sets 1 and 2 online). The size of the ellipses is roughly proportional to the number of gene transcripts affected (for more detailed information, see Supplemental Figure 8 online).

components that constitute or mediate the N/NO_3^- signal in higher plants. We successfully used a reverse genetic approach to investigate the potential functions of three strongly N/NO_3^--inducible members of the novel *LBD* gene family of TFs (Shuai et al., 2002; Scheible et al., 2004; Husbands et al., 2007). The three genes are highly related and most probably evolved by two subsequent segmental duplications of a chromosome 5 area comprising *LBD37* (http://www.tigr.org). Members of the plant-specific *LBD* TF gene family have been implicated in developmental processes during recent years (see Introduction), but for many *LBD* genes, functions are still unknown. Our results expand the knowledge about the *LBD* gene family by showing that some members are involved in regulation of metabolism. They mediate the N/NO_3^--dependent regulation of anthocyanin synthesis and also exert wider effects by repressing a larger number of N-responsive gene transcripts and key transcripts for NO_3^- assimilation, with subsequent alterations of N status and N-dependent growth (Figure 10). An important conclusion from our results is that expression of *LBD37*, *LBD38*, or *LBD39* constitutes an N availability signal in *Arabidopsis*.

LBD37, 38, and 39 Repress Anthocyanin Biosynthesis Upstream of *PAP1* and *PAP2*

The visual pigmentation phenotypes observed in *LBD37*, *LBD38*, and *LBD39* OX plants and the *lbd37*, *lbd38*, and *lbd39* mutants prompted us to perform a targeted analysis of flavonoid metabolism at the metabolite and transcript levels. All the results gathered suggest that these LBDs regulate the late anthocyanin-specific steps of flavonoid biosynthesis, thereby giving a striking phenocopy of the N/NO_3^- effect and a reverse phenocopy of *PAP1* OX on this part of secondary metabolism (Figure 6). *PAP1* and especially *PAP2* are strongly repressed in continuously N/NO_3^--fed *Arabidopsis* wild-type seedlings and in previously N-limited wild-type seedlings that were re-supplied with 3 mM KNO_3 for 3 h (Scheible et al., 2004). The same strong repression of *PAP1* and especially *PAP2* is observed in *LBD37* or *LBD38* OXs, suggesting that these LBDs are N/NO_3^--induced repressors acting upstream of *PAP1* and *PAP2* (Figure 10). Whether the LBDs can directly bind to *PAP1* and *PAP2* promoter regions remains to be investigated.

It is noteworthy that *LBD37* OX seedlings do not produce anthocyanins in leaves even when challenged with P limitation, high irradiation, and cold or high concentrations of sucrose (Figure 3G; see Supplemental Figure 2C online). In these conditions, *PAP2* remains strongly repressed, while *PAP1* is derepressed to the level present in the wild type (see Supplemental Figure 12 online). Thus, P deprivation, sucrose, light, and cold

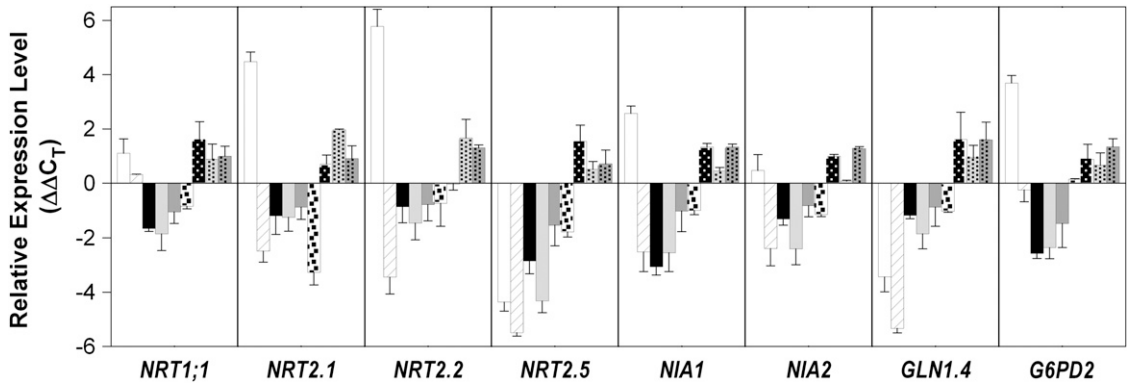

Figure 8. qRT-PCR Analysis of Gene Transcripts Involved in Nitrate Uptake and Assimilation.

Relative expression changes in (1) N-limited wild type after 3 h NO_3^- readdition versus N-limited wild type (white bar, 1st in each group), (2) NO_3^--fed versus N-limited wild types (hatched bar, 2nd in each group), (3) N-limited overexpressers of *LBD37*, *LBD38*, and *LBD39* versus N-limited wild types (black, light-gray, and medium-gray bars, respectively; 3rd to 5th in each group), (4) inducible *LBD37* overexpressers (iOX) after 3 h induction versus noninduced *LBD37* iOX (black dotted white bar, 6th in each group), and (5) N-replete *lbd37-1*, *lbd38*, and *lbd39* mutants versus N-replete wild type (white dotted black bar, black dotted light-gray bar, black dotted medium-gray bar, 7th to 9th in each group). Results represent mean values ± SD from three independent biological replicates/lines with two technical replicates for each. Note the logarithmic character of the data (cf. legend to Figure 1A).

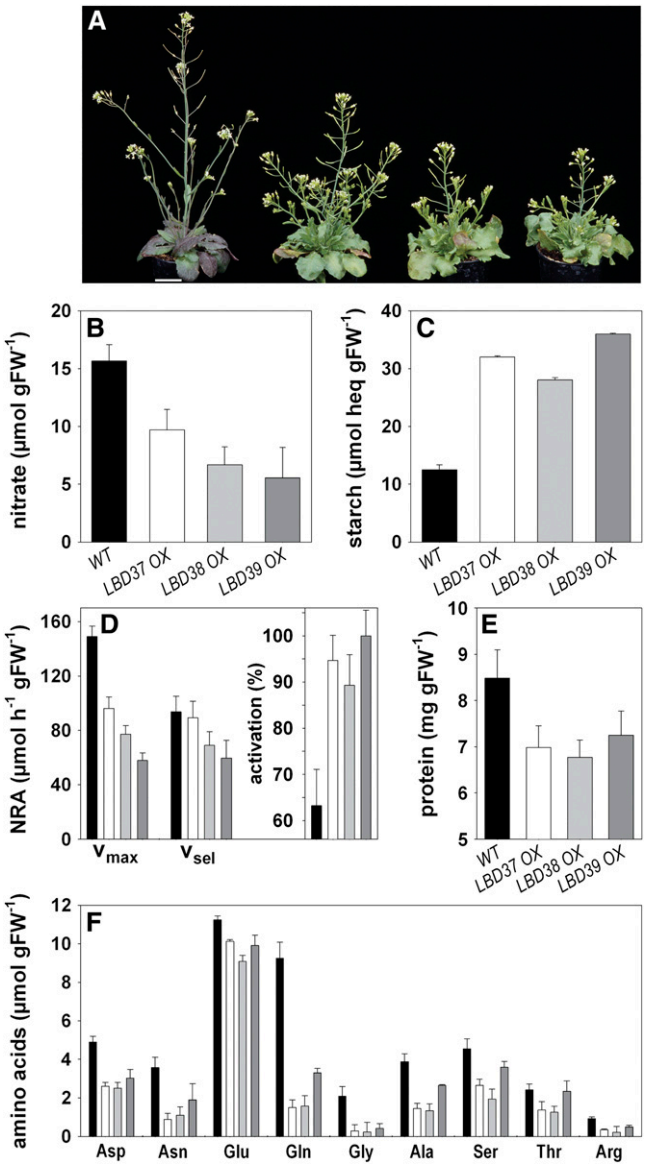

Figure 9. Altered N Status in *LBD* Overexpressors.

(A) Plant phenotype of the analyzed wild type, *LBD37*, *LBD38*, and *LBD39* OXs (from left to right). Bar = 2 cm.
(B) NO_3^- content.
(C) Starch content.
(D) Maximal and selective nitrate reductase activity, NRA, and NR activation (i.e., Vsel/Vmax).
(E) Protein content.
(F) Amino acid contents.
Results are from shoots of the plants shown in **(A)**. Wild type (black bars), *LBD37* (white bars), *LBD38* (light-gray bar), and *LBD39* OXs (medium-gray bars) were grown in high light conditions (cf. Figure 3H). Results are the average ± SD from three independent lines each. For each sample (i.e., line), materials from five individual plants were combined.

can antagonize the LBD-mediated N/NO_3^- repression of *PAP1* but not the repression of *PAP2* (Figure 10). Consistent with this, *PAP1* was proposed to have a key role in light and sucrose induction of anthocyanin biosynthesis in *Arabidopsis* (Teng et al., 2005; Solfanelli et al., 2006; Cominelli et al., 2008), whereas *PAP2* appears to be more important in the N/NO_3^- regulation of anthocyanin biosynthesis (Lea et al., 2007). The fact that *PAP1* expression in sugar- or P-stressed *LBD37* OX seedlings is still ~10-fold lower than in *PAP1*-overexpressing *pap1*-D lines (see Supplemental Figure 12 online) might explain their inability to produce high levels of anthocyanin.

OX of each *LBD* gene resulted in the same visual, physiological, and overall molecular phenotypes. Likewise, loss of function of each of the three *LBD* genes resulted in the reciprocal phenotypes. This shows that these putative paralogs have the same biological function and that reduced anthocyanins in *LBD* OX lines is not the result of ectopic expression. Also, analyses with ATTED II (Obayashi et al., 2007) or Gene-CAT (Mutwil et al., 2008) reveal coexpression of the three *LBD* genes, suggesting their involvement in the same biological process or possibly even the same molecular heteromeric complex, as exemplified for cellulose synthase isoforms (Taylor et al., 2003; Persson et al., 2007). The latter possibility is supported by the comparable phenotypes of each of the *lbd* single mutants and would suggest that LBD37, LBD38, and LBD39, although involved in the same biological process, have distinct or at least not fully redundant biochemical functions.

The data discussed so far provide evidence that the three LBDs regulate anthocyanin synthesis via repression of *PAP1* and *PAP2*. A number of other genes encoding MYB and bHLH TFs are known to be involved in regulating anthocyanin biosynthesis in seeds and vegetative tissues. The MYB and bHLH proteins form complexes with the TTG1 WD40-repeat protein in *Arabidopsis* and are able to regulate several epidermal gene expression programs in *Arabidopsis* (Broun, 2005), including the regulation of anthocyanin and proanthocyanin biosynthesis as well as mucilage synthesis in the seed coat or trichome and root hair organogenesis. Therefore, expression of additional *MYB* and *bHLH* TF genes, the *TTG1* gene, and a few other TF genes (e.g., *TT1* and *TTG2*) known to be involved in anthocyanin, procyanidin, flavonoid, or phenylpropanoid (e.g., MYB4) metabolism was analyzed. bHLH TT8 interacts with PAP1/PAP2 (Zimmermann

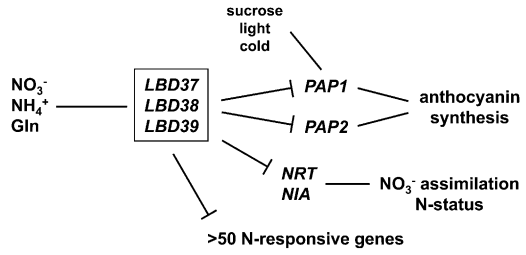

Figure 10. Model of LBD37, 38, and 39 Functions.

Major N sources induce *LBD37*, *38*, and *39*. Expression of these LBDs represses *PAP1* and *PAP2*, several important *NRT* and *NIA* genes, as well as a larger number of additional N-responsive genes, thereby decreasing anthocyanin synthesis, nitrate assimilation, and N status.

et al., 2004). *TT8* was found to be repressed by *LBD37* and *LBD38* OX and induced in *lbd37*, *lbd38*, and *lbd39* mutants and by *PAP1* OX. This illustrates coregulation of components of the same transcriptional complex and suggests *TT8* is not a direct target of LBD but that its expression rather depends on PAP1/PAP2. The closely related MYB11, MYB12, and MYB111 TFs are redundant positive regulators and affect flavonol accumulation in different parts of the *Arabidopsis* seedling by regulating several genes of flavonoid biosynthesis, including *CHS*, *CHI*, *F3H*, *FLS1*, and *UGT91A1* and *UGT84A1* (Stracke et al., 2007). Seedlings of the triple mutant *myb11 myb12 myb111* do not form flavonols, but accumulation of anthocyanins is unaffected in these seedlings (Stracke et al., 2007). In *LBD* OX seedlings, *MYB11* was repressed, but *MYB12* and *MYB111* were unchanged. Consistently, flavonols were also not affected. The small MYB protein *Arabidopsis* MYBL2 acts as a negative regulator (Dubos et al., 2008; Matsui et al., 2008). Loss of MYBL2 activity leads to strong anthocyanin accumulation and induction of late flavonoid biosynthesis genes as well as *TT8* and *PAP1*, while *MYBL2* overexpression suppressed these genes and inhibited the biosynthesis of proanthocyanidins in seeds. These results are analogous to what we observed with *LBD* OXs and mutants. It will be important to clarify the relationship and interaction between MYBL2 and the LBDs. The *TT1* gene encodes a nuclear WIP-domain zinc-finger protein that is involved in seed coat development and pigmentation (Sagasser et al., 2002). *LBD* OX lines and NO_3^--fed wild-types displayed strong induction of *TT1*, while it was strongly repressed by *PAP1* OX. The expression pattern of *TT1* is thus opposite to that of *PAP1*, *PAP2*, or the late flavonoid biosynthesis genes. Nothing is known about the function of this gene in vegetative tissue. There is no expression history available as it is not represented on ATH1 GeneChips and requires more sensitive methods, such as qRT-PCR, for detection in leaves. In conclusion, it is clear that the expression of some of these regulatory genes is modified in *LBD* OX lines, in *PAP1* OX, or by N/NO_3^-. However, it will require more work to determine whether these changes are direct or indirect and to finally clarify how the genes and their products interact.

The SPX-domain E3 ligase NLA was described to be required for anthocyanin production and other N limitation responses in *Arabidopsis* (Peng et al., 2007a, 2007b, 2008), as N-limited *nla* mutants no longer accumulate anthocyanin. Therefore, it is of interest to compare *nla* mutants and *LBD* OXs in more detail. In both genotypes, anthocyanin synthetic genes are repressed, but *nla* mutants do not show repression of *PAP1* or *PAP2* transcripts (Peng et al., 2007b), while this is a dominant transcriptional change in *LBD* OXs. The inability to produce anthocyanins also seems to occur only in mature *nla* mutant plants, as N-limited *nla* mutant seedlings display a wild-type-like anthocyanin pigmentation (see Supplemental Figure 2D online), while the three *LBD*s suppress anthocyanin production at the seedling stage already. Furthermore, the array of transcriptional changes observed in N-limited *nla* mutants and *LBD* OX lines is quite different, and neither is *NLA* transcript abundance affected in *LBD* OX lines, nor are *LBD37*, *38*, or *39* transcript levels altered in *nla* (see Supplemental Data Set 1 online and Peng et al., 2007b). These observations lead us to conclude that E3 ligase NLA and the LBDs affect anthocyanin production via different signaling pathways. LBDs appear to repress *PAP1*/*PAP2* transcription, whereas NLA possibly influences PAP1/PAP2 at a posttranslational level.

LBD37, 38, and 39 Expression in N-Limited Plants Mimics N Availability and Affects N-Dependent Traits

Inhibition of sectors of secondary metabolism is part of the primary response to NO_3^-/N (see Introduction). Repression of *LBD37*, *38*, and *39* during N limitation and rapid strong induction by NO_3^-, NH_4^+, or Gln as well as the fact that *LBD* OX inhibits anthocyanin synthesis and strongly represses *PAP1* and *PAP2* leads to the conclusion that the LBDs represent a primary component in a signaling pathway that represses anthocyanin production when NO_3^-/N is available (Figure 10). However, the range of traits altered by LBD expression is not limited to anthocyanins, as transcriptome studies revealed that a large majority of genes repressed in N-limited *LBD* OX lines are also repressed by NO_3^-/N availability. The LBDs influence the abundance of >50 or ~15% of the N-repressed transcripts in *Arabidopsis*, giving them broader importance in N signaling. An important role of these LBDs in N signaling and adaptation to changing NO_3^-/N availability can also be inferred from the observation that their transcripts are among the few that decrease when *Arabidopsis* plants are subjected to mild N limitation (A. Schlereth and M. Stitt, personal communication; see Tschoep et al. [2009] for the definition of mild N limitation).

Among the genes affected by the LBDs are the ones encoding nitrate reductase (*NIA*) and several NO_3^- transporters (*NRT*). *NIA* and some *NRT2* genes are induced as part of the primary response to NO_3^- (Redinbaugh and Campbell, 1991) and repressed by organic nitrogen sources such as Gln (Krapp et al., 1998; Lejay et al., 1999; Nazoa et al., 2003). *LBD* OX did not induce genes for NO_3^- uptake and assimilation; instead, OX of each of the three *LBD* genes led to a robust repression of *NIA* and several *NRT2* genes (Figure 8). The same was seen with *LBD* iOX lines, in which *NIA* and *NRT2* genes were repressed after ethanol induction (Figure 8; see Supplemental Figure 9A online). This indicates that, in contrast with NLP7, HY5, or NRT1.1 (see Introduction), the LBDs are not involved in the primary induction of N uptake and assimilation by NO_3^-. Fast and strong induction of the *LBDs* by NO_3^- also implies that the LBD proteins are synthesized, but de novo protein synthesis per se is not required for NO_3^- induction of *NIA* or *NRT2* genes (Redinbaugh and Campbell, 1991; Gowri et al., 1992). *NIA* or *NRT2* genes are also equally induced in N-limited wild-type and *lbd* mutants after NO_3^- readdition (see Supplemental Figure 9B online), providing yet more evidence that the LBDs are not involved in the primary induction of N uptake/assimilation by NO_3^-.

The best explanation for the observed repression of the genes involved in NO_3^- uptake and assimilation is that *LBD37-39* signal N availability to the plant system, leading to repression of specific N deficiency responses (like anthocyanin synthesis) and feedback repression of *NIA* or *NRT2* genes. The alternative view that *LBD37-39* expression could alter sugar signaling leading to repression of *NIA* or *NRT2* genes, which were described as being sugar inducible (Cheng et al., 1992; Lejay et al., 2003), seems unlikely as many of the gene transcripts repressed in LBD

OX seedlings and by N availability (e.g., *PAP2*, *NIA1*, *NRT2.1*, *NRT2.2*, *At1g74810*, *At1g22160*, *At5g02580*, *At5g02230*, *At3g62960*, and *At1g76960*; see Supplemental Data Set 1 online; Scheible et al., 2004) are much less affected or not affected by sugars (cf. data from Osuna et al., 2007). Conversely, strongly sugar-responsive genes in *Arabidopsis* seedlings (Osuna et al., 2007) are hardly or not affected in LBD OX seedlings.

Mimicry of N availability by *LBD* expression, the resulting repression of *NIA* and *NRT2* genes, and reduction of NO_3^- assimilation will eventually affect plant N status. Consistently, mature soil-grown *LBD* OX plants have a low NO_3^- content and a shortage of organic N compounds (most notably a reduction of Gln, but also protein content). Other typical indicators of low N status observed in the *LBD* OX plants are high activation (90 to 100%) of NR (Scheible et al., 1997b, 1997c) and starch accumulation (Scheible et al., 1997a; Peng et al., 2007a). Mimicry of N availability by *LBD* expression can also be deduced from the alteration of basal shoot branching, an N-dependent growth phenotype (see Supplemental Figure 11 online; Crawford and Forde, 2002; Médiène et al., 2002). Shoot branching has long been known to be influenced by hormones such as cytokinins and auxin (for review, see Ongaro and Leyser, 2008) and recently also by strigolactones (Gomez-Roldan et al., 2008; Umehara et al., 2008). It is also known that cytokinins are produced in response to NO_3^- addition in *Arabidopsis* roots (Takei et al., 2002) and move acropetally and promote shoot branching. It will be interesting to establish whether the LBDs affect the levels or the transport of these hormones too.

In conclusion, the identification of the three *LBDs* as regulators of anthocyanin synthesis and repressors of a larger number of N-repressed gene transcripts pinpoints these *LBD* genes as important molecular components in plant NO_3^-/N signaling.

METHODS

Plant Genotypes

Arabidopsis thaliana wild-type Columbia-0 seeds were obtained from an MPI-MP in-house collection. *LBD* gene T-DNA insertion lines (*lbd37-1*, *SALK_097991*; *lbd37-2*, *SALK_057939*; *lbd39*, *SALK_049910*) and the activation-tagging mutant *pap1-D* (Borevitz et al., 2000) were obtained through the Nottingham Arabidopsis Stock Centre (NASC). The T-DNA insertion line *lbd38* (*GABI_049C12*) was generated in the context of the GABI-Kat program and provided by Bernd Weisshaar (MPI for Plant Breeding Research, Cologne, Germany). Seeds of *nia1nia2* double mutants (Wang et al., 2004) were provided by Marc Lepetit (Institute for Integrative Plant Biology, Montpellier, France).

Homozygous T-DNA insertion lines were identified by standard PCR procedures with wild-type and T-DNA–specific primer pairs (*lbd37-1*: FwdP 5′-TCGTCCAATATACTGGTTGGAATTT-3′ and RevP 5′-TCCAGCAAAATGATTCCACCG-3′; *lbd37-2*: FwdP 5′-TTGGTCCAACCACATGCTTA-3′ and RevP 5′-TCTCCAGCAAAATGATTCCAC-3′; *lbd38*: FwdP 5′-GGAGATAGAACCATGAGTTGCAATGGTTGTCGA-3′ and RevP 5′-CAAGAAAGCTGGGTCTCAAGCGAAGAGATTGAGCAA-3′; *lbd39*: FwdP 5′-ATCTTTGAGTGTTTTGCGTCG and RevP 5′-TTCGGAAAAGAAATGAGTTGC-3′). To amplify T-DNA–specific products, RevP primers were combined with LBb2 (5′-GCGTGGACCGCTTGCTGCAACT-3′) for *lbd37_1* and *lbd37_2* or with LBc1 (5′-CCGCAATGTGTTATTAAGTTG-3′) for *lbd39*. The *lbd38* primer, RevP2 (5′-AAGAGATTGAGCAACTTTGTCGTT-3′), was combined with the GabiKat-LB-primer (5′-CCCATTTGGACGTGAATGTAGACAC-3′).

For production of constitutive and inducible *LBD* OX and *GFP-LBD* fusion constructs, PCR fragments containing the entire annotated *LBD* coding sequences were amplified from cDNA pools, directionally cloned into GATEWAY entry vector pENTRY/SD/D-TOPO (Invitrogen), transferred by homologous recombination into destination vector pMDC32 (Curtis and Grossniklaus, 2003), pSRN (Junker et al., 2003), or pK7FWG2 (Karimi et al., 2002), and finally transformed into wild-type Columba-0 via *Agrobacterium tumefaciens* GV3101 (Clough and Bent, 1998).

Plant Growth Conditions

Wild-type, T-DNA mutant, and OX lines were grown on GS90 soil (100% N; 0.3 g NH_4NO_3 L^{-1}) (Gebrüder Patzer), 0% N soil (GS90 N-free), or 50% N soil (1:1 mixture of the two soil types) in Percival AR-36L growth chambers (Percival Scientific) in a 16-h-light (~150 μE, 20°C)/8-h-dark (18°C) or 24-h-light cycle at ~70% relative humidity. For high-light conditions, the wild type and OXs were grown on GS90 soil for 4 weeks and then transferred to a Percival chamber with 8 h light (600 μE, 20°C)/16 h dark (18°C) at ~70% relative humidity. Samples were taken in the middle of the light period.

Arabidopsis seedlings were grown in sterile liquid culture (Scheible et al., 2004) either for 9 d in N-replete conditions (FN, 4 mM KNO_3) or first for 7 d in FN and then for 2 d in N deprivation conditions (no N added; −N). On day 9, some batches of N-starved seedlings were resupplied with 3 mM KNO_3 for 30 min or 3 h (wild type and mutants) or treated with 0.2% ethanol for 3 and 6 h (iOX). For additional stress conditions, seedlings were grown for 7 d in FN and another 3 d in N or P deprivation conditions (Morcuende et al., 2007), high concentrations of sucrose (6% w/v), or transferred to the cold (4°C). For that purpose, seedlings were pregrown in 24 h light (150 to 180 μE, 20°C) on sterile 0.5% (w/v) agar plates (Falcon Integrid 100 mm square) containing 27 mL FN medium, and after 7 d, seedlings were transferred individually to 24-well culture plates (Greiner Bio-one Cellstar 662160) containing 1 mL of medium per well.

Quantitative Real-time PCR

All steps including RNA isolation, cDNA synthesis, quality control, primer design, real-time PCR, and data analysis were performed as described (Czechowski et al., 2004, 2005; Udvardi et al., 2008). Sequences and amplification efficiencies (E) of qRT-PCR primers are listed in Supplemental Table 1 online.

Affymetrix ATH1 GeneChip Experiments

Total RNA was prepared separately from three biological replicates of N-limited *LBD37*OX, *LBD38*OX, and wild-type seedlings and N-replete *lbd37-1* mutant, *lbd38* mutant, and wild-type seedlings (i.e., 18 samples) using a Qiagen RNeasy plant mini kit. RNA concentration was measured with a NanoDrop ND-1000 UV-Vis spectrophotometer (Nanodrop Technologies). Subsequent procedures, including (1) quality controls of RNA, (2) preparation and biotin labeling of cRNA, (3) ATH1 GeneChip hybridizations, washing, staining, and scanning, were performed by ATLAS Biolabs. Processing of ATH1 GeneChip raw data (CEL files) was performed with open source ROBIN software (http://mapman.gabipd.org), which provides a user-friendly interface to powerful microarray processing. First, the CEL files were processed with RMA (log-scale robust multiarray analysis) based on Quantile normalization (Irizarry et al., 2003). Subsequently, a linear model was fitted using the R limma package (Smyth, 2004) and the contrasts (1) wild-type FN versus wild-type –N wild-type, (2) LBD37 OX –N versus wild-type –N, (3) LBD38 OX –N versus wild-type –N, as well as (4 and 5) *lbd37* FN and *lbd38* FN versus wild-type FN were extracted. P values were estimated using the empirical Bayes procedure implemented in limma. Differential expression across different

comparisons was assessed by identifying genes having a false discovery rate below 5% using multiple testing adjustment (Benjamini and Hochberg, 1995) and identifying significant contrasts using the nestedF procedure in limma. The RMA-normalized log2 signal intensities for all 22,750 ATH1 probe sets from 18 arrays, the log2 fold changes, and adjusted P values for probe sets with ≥2-fold differential signal intensity are compiled in Supplemental Data Sets 1 and 2 online. Data and Affymetrix CEL-files are also accessible at the National Center for Biotechnology Information Gene Expression Omnibus database (Edgar et al., 2002) under accession number GSE18818.

Nonradioactive RNA Gel Blot Analysis

Total RNA was isolated from constitutive and inducible *LBD* OX lines or *lbd37-1* mutants, and 10-μg aliquots were loaded on a formaldehyde-containing 1.5% (w/v) agarose gel and electrophoretically separated. For hybridization, digoxigenin-labeled PCR products (encoding gene-specific regions of each *LBD* gene) were used and detected by chemiluminescence using CDPStar reagent (New England Biolabs). Details are described by Peterhaensel et al. (1998).

Targeted Flavonoid Profiling

Shoot material from three biological replicates of freeze-dried 9-d-old seedlings of N-limited and N-replete LBD37OX, LBD38OX (two independent lines each), and wild-type seedlings, and N-sufficient *lbd37-1*, *lbd37-2*, *lbd38*, *lbd39*, and *lbd38 lbd39* mutants and wild-type seedlings (~20 mg fresh weight) were homogenized in five volumes of 50% methanol. Two-microliter aliquots were subjected to liquid chromatography–electrospray ionization–mass spectrometry analysis. Extraction and analysis of flavonoid pathway intermediates was performed as described previously (Tohge et al., 2005; Matsuda et al., 2009).

Lignin Staining

Inflorescence stems of 4-week-old plants grown on FN agar (0.5% w/v) plates were harvested, and 50-μm cross sections were cut from stems pieces of equal developmental age. Sections were put on a microscope slide and treated with one to two drops of freshly prepared phloroglucinol solution (25 mg phloroglucinol dissolved in 25 mL 100% ethanol and 25 mL 37% hydrochloric acid). After incubation for 5 min, the sections were observed using a Leica MZ 12.5 stereomicroscope, and photomicrographs were taken with a mounted digital camera system.

Determination of Nitrate, Nitrate Reductase Activity, Amino Acids, Protein, and Starch

Metabolites were extracted twice with 80% ethanol and once with 50% ethanol from shoot tissue of three biological replicates each pooled from five individual *LBD37OX*, *LBD38OX*, *LBD39OX*, and wild-type plants grown in high light conditions (600 μE) or 9-d-old N-sufficient *lbd* mutant and wild-type seedlings. The same ethanolic extracts were used for determination of nitrate, nitrate reductase activity, amino acids, protein, and starch. Details are described by Cross et al. (2006), Gibon et al. (2004), and Hendriks et al. (2003).

Accession Numbers

Sequence data from this article can be found in the Arabidopsis Genome Initiative or GenBank/EMBL databases under AT5G67420 (*LBD37*), AT3G49940 (*LBD38*), AT4G37540 (*LBD39*), and the accession numbers compiled in Supplemental Table 1 online.

Author Contributions

G.R. and W.-R.S. designed the research and analyzed data. G.R. performed the research. T.T. and F.M. measured flavonoids and analyzed flavonoid profiling data. F.M. and K.S. contributed tools and equipment for flavonoid analysis. W.-R.S. wrote the article.

Supplemental Data

The following materials are available in the online version of this article.

Supplemental Figure 1. N/NO_3^--Specific, Strong Induction of *LBD37*, *LBD38*, and *LBD39.*

Supplemental Figure 2. Anthocyanin Pigmentation Phenotypes.

Supplemental Figure 3. Nuclear Localization of LBD37-GFP Fusion Protein.

Supplemental Figure 4. Flavonoid Levels and Lignin Staining.

Supplemental Figure 5. Expression of Late Flavonoid Pathway Genes and Regulators in *lbd37*, *lbd38*, and *lbd39* Mutants.

Supplemental Figure 6. qRT-PCR Transcript Profiling of Early Flavonoid Pathway Genes and Regulators.

Supplemental Figure 7. Expression of Flavonoid Pathway Genes and Regulators in Inducible *LBD37* Overexpressor Lines.

Supplemental Figure 8. Comparison of Transcriptome Changes in Response to Nitrogen Status and *LBD37* or *LBD38* Overexpression.

Supplemental Figure 9. Expression of *NRT2.1* and *NIA* Genes in *LBD37* iOX Lines and *lbd* Mutant Seedlings.

Supplemental Figure 10. Amino Acid Levels in *lbd* Mutant Seedlings.

Supplemental Figure 11. Nitrogen-Dependent Basal Shoot Branching Phenotype.

Supplemental Figure 12. Expression of *PAP1* and *PAP2* in *LBD37* Overexpressers during Environmental Stress Conditions.

Supplemental Table 1. Accession Numbers and Primer Sequences for (Semi-) Quantitative RT-PCR.

Supplemental Data Set 1. ATH1 GeneChip Results for Wild-Type and *LBD* Overexpressers.

Supplemental Data Set 2. ATH1 GeneChip Results for Wild-Type and *lbd* Mutants.

ACKNOWLEDGMENTS

The work was supported by the Max-Planck Society. We thank our former and present colleagues Tomasz Czechowski, Jens-Holger Dieterich, Regina Feil, Yves Gibon, John Lunn, Rosa Morcuende, Magdalena Musialak-Lange, Armin Schlereth, Mark Stitt, Michael Udvardi, and Pia Walch-Liu for valuable input, help, discussions, and suggestions on the manuscript. Thanks also to Björn Usadel and Marc Lohse for implementing ROBIN, the software for processing and statistical treatment of the ATH1 GeneChip data. We also thank Josef Bergstein and Eugenia Maximova (Max-Planck Institute for Molecular Plant Physiology) for providing photographical and microscopy expertise. The SALK and Gabi-Kat consortia and ABRC/NASC are acknowledged for generating and providing T-DNA insertion lines. Finally, we also express our gratitude to Marc Lepetit (Institute for Integrative Plant Biology, Montpellier, France) and Steven J. Rothstein (University of Guelph, Ontario, Canada) for providing *nia1 nia2* and *nla* mutant seeds, respectively.

Received March 16, 2009; revised October 21, 2009; accepted October 31, 2009; published November 20, 2009.

REFERENCES

Addo-Quaye, C., Eshoo, T.W., Bartel, D.P., and Axtell, M.J. (2008). Endogenous siRNA and miRNA targets identified by sequencing of the Arabidopsis degradome. Curr. Biol. **18:** 758–762.

Alboresi, A., Gestin, C., Leydecker, M.T., Bedu, M., Meyer, C., and Truong, H.N. (2005). Nitrate, a signal relieving seed dormancy in Arabidopsis. Plant Cell Environ. **28:** 500–512.

Alonso, J.M., Stepanova, A.N., Leisse, T.J., Kim, C.J., Chen, H., Shinn, P., Stevenson, D.K., Zimmerman, J., Barajas, P., Cheuk, R., Gadrinab, C., and Heller, C. (2003). Genome-wide insertional mutagenesis of *Arabidopsis thaliana.* Science **301:** 653–657.

Benjamini, Y., and Hochberg, Y. (1995). Controlling the false discovery rate: A practical and powerful approach to multiple testing. J. R. Stat. Soc., B **57:** 289–300.

Bernier, G., Havelange, A., Houssa, C., Petitjean, A., and Lejeune, P. (1993). Physiological signals that induce flowering. Plant Cell **5:** 1147–1155.

Borevitz, J.O., Xia, Y., Blount, J., Dixon, R.A., and Lamb, C. (2000). Activation tagging identifies a conserved MYB regulator of phenylpropanoid biosynthesis. Plant Cell **12:** 2383–2394.

Borghi, L., Bureau, M., and Simon, R. (2007). Arabidopsis JAGGED LATERAL ORGANS is expressed in boundaries and coordinates KNOX and PIN activity. Plant Cell **19:** 1795–1808.

Bortiri, E., Chuck, G., Vollbrecht, E., Rocheford, T., Martienssen, R., and Hake, S. (2006). ramosa2 encodes a LATERAL ORGAN BOUNDARY domain protein that determines the fate of stem cells in branch meristems of maize. Plant Cell **18:** 574–585.

Broun, P. (2005). Transcriptional control of flavonoid biosynthesis: A complex network of conserved regulators involved in multiple aspects of differentiation in Arabidopsis. Curr. Opin. Plant Biol. **8:** 272–279.

Byrne, M.E., Simorowski, J., and Martienssen, R.A. (2002). ASYMMETRIC LEAVES1 reveals knox gene redundancy in Arabidopsis. Development **129:** 1957–1965.

Castaings, L., Camargo, A., Pocholle, D., Gaudon, V., Texier, Y., Boutet-Mercey, S., Taconnat, L., Renou, J.P., Daniel-Vedele, F., Fernandez, E., Meyer, C., and Krapp, A. (2009). The nodule inception-like protein 7 modulates nitrate sensing and metabolism in Arabidopsis. Plant J. **57:** 426–435.

Chalfun-Junior, A., Franken, J., Mes, J.J., Marsch-Martinez, N., Pereira, A., and Angenent, G.C. (2005). ASYMMETRIC LEAVES2-LIKE1 gene, a member of the AS2/LOB family, controls proximal-distal patterning in Arabidopsis petals. Plant Mol. Biol. **57:** 559–575.

Chen, Z.H., Jenkins, G.I., and Nimmo, H.G. (2008). Identification of an F-box protein that negatively regulates P(i) starvation responses. Plant Cell Physiol. **49:** 1902–1906.

Chen, Z.H., Nimmo, G.A., Jenkins, G.I., and Nimmo, H.G. (2007). BHLH32 modulates several biochemical and morphological processes that respond to Pi starvation in Arabidopsis. Biochem. J. **405:** 191–198.

Cheng, C.L., Acedo, G.N., Christinsin, M., and Conkling, M. (1992). Sucrose mimics the light induction of Arabidopsis nitrate reductase gene transcription. Proc. Natl. Acad. Sci. USA **89:** 1861–1864.

Clough, S.J., and Bent, A.F. (1998). Floral dip: A simplified method for *Agrobacterium*-mediated transformation of *Arabidopsis thaliana.* Plant J. **16:** 735–743.

Cominelli, E., Gusmaroli, G., Allegra, D., Galbiati, M., Wade, H.K., Jenkins, G.I., and Tonelli, C. (2008). Expression analysis of anthocyanin regulatory genes in response to different light qualities in *Arabidopsis thaliana*. J. Plant Physiol. **165:** 886–894.

Crawford, N.M. (1995). Nitrate: Nutrient and signal for plant growth. Plant Cell **7:** 859–868.

Crawford, N.M., and Forde, B.G. (2002). Molecular and developmental biology of inorganic nitrogen nutrition. In The Arabidopsis Book, C.R. Somerville and E.M. Meyerowitz, eds (Rockville, MD: American Society of Plant Biologists), doi/http://www.aspb.org/publications/arabidopsis/.

Cross, J.M., von Korff, M., Altmann, T., Bartzetko, L., Sulpice, R., Gibon, Y., Palacios, N., and Stitt, M. (2006). Variation of enzyme activities and metabolite levels in 24 Arabidopsis accessions growing in carbon-limited conditions. Plant Physiol. **142:** 1574–1588.

Curtis, M.D., and Grossniklaus, U. (2003). A gateway cloning vector set for high-throughput functional analysis of genes in planta. Plant Physiol. **133:** 462–469.

Czechowski, T., Bari, R.P., Stitt, M., Scheible, W.-R., and Udvardi, M.K. (2004). Real-time RT-PCR profiling of over 1400 Arabidopsis transcription factors: Unprecedented sensitivity reveals novel root- and shoot-specific genes. Plant J. **38:** 366–379.

Czechowski, T., Stitt, M., Altmann, T., Udvardi, M.K., and Scheible, W.-R. (2005). Genome-wide identification and testing of superior reference genes for transcript normalization in Arabidopsis. Plant Physiol. **139:** 5–17.

Dixon, R.A., and Paiva, N.L. (1995). Stress-induced phenylpropanoid metabolism. Plant Cell **7:** 1085–1097.

Dubos, C., Le Gourrierec, J., Baudry, A., Huep, G., Lanet, E., Debeaujon, I., Routaboul, J.M., Alboresi, A., Weisshaar, B., and Lepiniec, L. (2008). MYBL2 is a new regulator of flavonoid biosynthesis in *Arabidopsis thaliana*. Plant J. **55:** 940–953.

Edgar, R., Domrachev, M., and Lash, A.E. (2002). Gene expression omnibus: NCBI gene expression and hybridization array data repository. Nucleic Acids Res. **30:** 207–210.

Evans, M.M. (2007). The indeterminate gametophyte1 gene of maize encodes a LOB domain protein required for embryo Sac and leaf development. Plant Cell **19:** 46–62.

Fritz, C., Palacios-Rojas, N., Feil, R., and Stitt, M. (2006). Regulation of secondary metabolism by the carbon-nitrogen status in tobacco: Nitrate inhibits large sectors of phenylpropanoid metabolism. Plant J. **46:** 533–548.

Gibon, Y., Blaesing, O.E., Hannemann, J., Carillo, P., Höhne, M., Hendriks, J.H., Palacios, N., Cross, J., Selbig, J., and Stitt, M. (2004). A Robot-based platform to measure multiple enzyme activities in *Arabidopsis* using a set of cycling assays: Comparison of changes of enzyme activities and transcript levels during diurnal cycles and in prolonged darkness. Plant Cell **16:** 3304–3325.

Gomez-Roldan, V., et al. (2008). Strigolactone inhibition of shoot branching. Nature **455:** 189–194.

Gould, K.S., McKelvie, J., and Markham, K.R. (2002). Do anthocyanins function as antioxidants in leaves? Imaging of H2O2 in red and green leaves after mechanical injury. Plant Cell Environ. **25:** 1261–1269.

Gowri, G., Kenis, J.D., Ingemarsson, B., Redinbaugh, M.G., and Campbell, W.H. (1992). Nitrate reductase transcript is expressed in the primary response of maize to environmental nitrate. Plant Mol. Biol. **18:** 55–64.

Guo, F.Q., Young, J., and Crawford, N.M. (2003). The nitrate transporter AtNRT1.1 (CHL1) functions in stomatal opening and contributes to drought susceptibility in *Arabidopsis*. Plant Cell **15:** 107–117.

Hendriks, J.H., Kolbe, A., Gibon, Y., Stitt, M., and Geigenberger, P. (2003). ADP-glucose pyrophosphorylase is activated by posttranslational redox-modification in response to light and to sugars in leaves of Arabidopsis and other plant species. Plant Physiol. **133:** 838–849.

Hoch, W.A., Singsaas, E.L., and McCown, B.H. (2003). Resorption protection. Anthocyanins facilitate nutrient recovery in autumn by shielding leaves from potentially damaging light levels. Plant Physiol. **133:** 1296–1305.

Hu, H.C., Wang, Y.Y., and Tsay, Y.F. (2009). AtCIPK8, a CBL-interacting protein kinase, regulates the low-affinity phase of the primary nitrate response. Plant J. **57:** 264–278.

Husbands, A., Bell, E.M., Shuai, B., Smith, H.M., and Springer, P.S. (2007). LATERAL ORGAN BOUNDARIES defines a new family of DNA-binding transcription factors and can interact with specific bHLH proteins. Nucleic Acids Res. **35:** 6663–6671.

Irizarry, R.A., Hobbs, B., Collin, F., Beazer-Barclay, Y.D., Antonellis, K.J., Scherf, U., and Speed, T.P. (2003). Exploration, normalization, and summaries of high density oligonucleotide array probe level data. Biostatistics **4:** 249–264.

Jonassen, E.M., Sévin, D.C., and Lillo, C. (June 17, 2009). The bZIP transcription factors HY5 and HYH are positive regulators of the main nitrate reductase gene in Arabidopsis leaves, *NIA2*, but negative regulators of the nitrate uptake gene *NRT1.1*. J. Plant Physiol. **166:** 2071–2076.

Junker, B.H., Chu, C., Sonnewald, U., Willmitzer, L., and Fernie, A.R. (2003). In plants the alc gene expression system responds more rapidly following induction with acetaldehyde than with ethanol. FEBS Lett. **535:** 136–140.

Karimi, M., Inze, D., and Depicker, A. (2002). GATEWAY vectors for Agrobacterium-mediated plant transformation. Trends Plant Sci. **7:** 193–195.

Krapp, A., Fraisier, V., Scheible, W.R., Quesada, A., Gojon, A., Stitt, M., Caboche, M., and Daniel-Vedele, F. (1998). Expression studies of Nrt2:1Np, a putative high-affinity nitrate transporter: evidence for its role in nitrate uptake. Plant J. **14:** 723–731.

Lea, U., Slimestad, R., Smedvig, P., and Lillo, C. (2007). Nitrogen deficiency enhances expression of specific MYB and bHLH transcription factors and accumulation of end products in the flavonoid pathway. Planta **225:** 1245–1253.

Lejay, L., Gansel, X., Cerezo, M., Tillard, P., Müller, C., Krapp, A., von Wirén, N., Daniel-Vedele, F., and Gojon, A. (2003). Regulation of root ion transporters by photosynthesis: Functional importance and relation with hexokinase. Plant Cell **15:** 2218–2232.

Lejay, L., Tillard, P., Lepetit, M., Olive, F., Filleur, S., Daniel-Vedele, F., and Gojon, A. (1999). Molecular and functional regulation of two NO3- uptake systems by N- and C-status of Arabidopsis plants. Plant J. **18:** 509–519.

Lillo, C., Lea, U.S., and Ruoff, P. (2008). Nutrient depletion as a key factor for manipulating gene expression and product formation in different branches of the flavonoid pathway. Plant Cell Environ. **31:** 587–601.

Lin, W.C., Shuai, B., and Springer, P.S. (2003). The *Arabidopsis* LATERAL ORGAN BOUNDARIES-domain gene ASYMMETRIC LEAVES2 functions in the repression of KNOX gene expression and in adaxial-abaxial patterning. Plant Cell **15:** 2241–2252.

Little, D.Y., Rao, H., Oliva, S., Daniel-Vedele, F., Krapp, A., and Malamy, J.E. (2005). The putative high-affinity nitrate transporter NRT2.1 represses lateral root initiation in response to nutritional cues. Proc. Natl. Acad. Sci. USA **102:** 13693–13698.

Matsuda, F., Yonekura-Sakakibara, K., Niida, R., Kuromori, T., Shinozaki, K., and Saito, K. (2009). MS/MS spectral tag-based annotation of non-targeted profile of plant secondary metabolites. Plant J. **57:** 555–577.

Matsui, K., Umemura, Y., and Ohme-Takagi, M. (2008). AtMYBL2, a protein with a single MYB domain, acts as a negative regulator of anthocyanin biosynthesis in Arabidopsis. Plant J. **55:** 954–967.

Médiène, S., Pagès, L., Jordan, M.-O., Le Bot, J., and Adamowicz, S. (2002). Influence of nitrogen availability on shoot development in young peach trees *Prunus persica* (L.) Batsch. Trends Ecol. Evol. **16:** 547–554.

Mehrtens, F., Kranz, H., Bednarek, P., and Weisshaar, B. (2005). The Arabidopsis transcription factor MYB12 is a flavonol-specific regulator of phenylpropanoid biosynthesis. Plant Physiol. **138:** 1083–1096.

Morcuende, R., Bari, R., Gibon, Y., Zheng, W., Pant, B.D., Blasing, O., Usadel, B., Czechowski, T., Udvardi, M.K., Stitt, M., and Scheible, W.-R. (2007). Genome-wide reprogramming of metabolism and regulatory networks of Arabidopsis in response to phosphorus. Plant Cell Environ. **30:** 85–112.

Muños, S., Cazettes, C., Fizames, C., Gaymard, F., Tillard, P., Lepetit, M., Lejay, L., and Gojon, A. (2004). Transcript profiling in the chl1-5 mutant of *Arabidopsis* reveals a role of the nitrate transporter NRT1.1 in the regulation of another nitrate transporter, NRT2.1. Plant Cell **16:** 2433–2447.

Mutwil, M., Obro, J., Willats, W.G., and Persson, S. (2008). GeneCAT – Novel webtools that combine BLAST and co-expression analyses. Nucleic Acids Res. **36:** W320–326.

Nagata, T., Todoriki, S., Masumizu, T., Suda, I., Furuta, S., Du, Z., and Kikuchi, S. (2003). Levels of active oxygen species are controlled by ascorbic acid and anthocyanin in Arabidopsis. J. Agric. Food Chem. **51:** 2992–2999.

Nazoa, P., Vidmar, J.J., Tranbarger, T.J., Mouline, K., Damiani, I., Tillard, P., Zhuo, D., Glass, A.D.M., and Touraine, B. (2003). Regulation of the nitrate transporter gene AtNRT2.1 in *Arabidopsis thaliana*: Responses to nitrate, amino acids and developmental stage. Plant Mol. Biol. **52:** 689–703.

Nesi, N., Debeaujon, I., Jond, C., Pelletier, G., Caboche, M., and Lepiniec, L. (2000). The TT8 gene encodes a basic helix-loop-helix domain protein required for expression of DFR and BAN genes in *Arabidopsis* siliques. Plant Cell **12:** 1863–1878.

Nesi, N., Jond, C., Debeaujon, I., Caboche, M., and Lepiniec, L. (2001). The Arabidopsis TT2 gene encodes an R2R3 MYB domain protein that acts as a key determinant for proanthocyanidin accumulation in developing seed. Plant Cell **13:** 2099–2114.

Nilsson, L., Müller, R., and Nielsen, T.H. (2007). Increased expression of the MYB-related transcription factor, PHR1, leads to enhanced phosphate uptake in *Arabidopsis thaliana*. Plant Cell Environ. **30:** 1499–1512.

Obayashi, T., Kinoshita, K., Nakai, K., Shibaoka, M., Hayashi, S., Saeki, M., Shibata, D., Saito, K., and Ohta, H. (2007). ATTED-II: A database of co-expressed genes and cis elements for identifying co-regulated gene groups in Arabidopsis. Nucleic Acids Res. **35:** D863–D869.

Okushima, Y., Fukaki, H., Onoda, M., Theologis, A., and Tasaka, M. (2007). ARF7 and ARF19 regulate lateral root formation via direct activation of LBD/ASL genes in Arabidopsis. Plant Cell **19:** 118–130.

Ongaro, V., and Leyser, O. (2008). Hormonal control of shoot branching. J. Exp. Bot. **59:** 67–74.

Ori, N., Eshed, Y., Chuck, G., Bowman, J.L., and Hake, S. (2000). Mechanisms that control knox gene expression in the Arabidopsis shoot. Development **127:** 5523–5532.

Osuna, D., Usadel, B., Morcuende, R., Gibon, Y., Bläsing, O.E., Hohne, M., Gunter, M., Kamlage, B., Trethewey, R., Scheible, W. R., and Stitt, M. (2007). Temporal responses of transcripts, enzyme activities and metabolites after adding sucrose to carbon-deprived Arabidopsis seedlings. Plant J. **49:** 463–491.

Peng, M., Bi, Y.M., Zhu, T., and Rothstein, S.J. (2007b). Genome-wide analysis of Arabidopsis responsive transcriptome to nitrogen limitation and its regulation by the ubiquitin ligase *NLA.* Plant Mol. Biol. **65:** 775–797.

Peng, M., Hannam, C., Gu, H., Bi, Y.M., and Rothstein, S.J. (2007a). A mutation in NLA, which encodes a RING-type ubiquitin ligase, disrupts the adaptability of Arabidopsis to nitrogen limitation. Plant J. **50:** 320–337.

Peng, M., Hudson, D., Schofield, A., Tsao, R., Yang, R., Gu, H., Bi, Y. M., and Rothstein, S.J. (2008). Adaptation of Arabidopsis to nitrogen

limitation involves induction of anthocyanin synthesis which is controlled by the NLA gene. J. Exp. Bot. **59:** 2933–2944.

Persson, S., Paredez, A., Carroll, A., Palsdottir, H., Doblin, M., Poindexter, P., Khitrov, N., Auer, M., and Somerville, C.R. (2007). Genetic evidence for three unique components in primary cell-wall cellulose synthase complexes in Arabidopsis. Proc. Natl. Acad. Sci. USA **104:** 15566–15571.

Peterhaensel, C., Obermaier, I., and Rueger, B. (1998). Nonradioactive Northern blot analysis of plant RNA and the application of different haptens for reprobing. Anal. Biochem. **264:** 279–283.

Redinbaugh, M.G., and Campbell, W.H. (1991). Higher plant responses to environmental nitrate. Physiol. Plant. **82:** 640–650.

Remans, T., Nacry, P., Pervent, M., Filleur, S., Diatloff, E., Mounier, E., Tillard, P., Forde, B.G., and Gojon, A. (2006). The Arabidopsis NRT1.1 transporter participates in the signaling pathway triggering root colonization of nitrate-rich patches. Proc. Natl. Acad. Sci. USA **103:** 19206–19211.

Rosso, M.G., Li, Y., Strizhov, N., Reiss, B., Dekker, K., and Weisshaar, B. (2003). An *Arabidopsis thaliana* T-DNA mutagenized population (GABI-Kat) for flanking sequence tag-based reverse genetics. Plant Mol. Biol. **53:** 247–259.

Sagasser, M., Lu, G.-H., Hahlbrock, K., and Weisshaar, B. (2002). *A. thaliana* TRANSPARENT TESTA 1 is involved in seed coat development and defines the WIP subfamily of plant zinc finger proteins. Genes Dev. **16:** 138–149.

Scheible, W.-R., Gonzalez-Fontes, A., Lauerer, M., Muller-Rober, B., Caboche, M., and Stitt, M. (1997a). Nitrate acts as a signal to induce organic acid metabolism and repress starch metabolism in tobacco. Plant Cell **9:** 783–798.

Scheible, W.-R., González-Fontes, A., Morcuende, R., Lauerer, M., Geiger, M., Glaab, J., Gojon, A., Schulze, E.-D., and Stitt, M. (1997c). Tobacco mutants with a decreased number of functional nia genes compensate by modifying the diurnal regulation of transcription, post-translational modification and turnover of nitrate reductase. Planta **203:** 304–319.

Scheible, W.-R., Lauerer, M., Schulze, E.D., Caboche, M., and Stitt, M. (1997b). Accumulation of nitrate in the shoot acts as a signal to regulate shoot-root allocation in tobacco. Plant J. **11:** 671–691.

Scheible, W.-R., Morcuende, R., Czechowski, T., Fritz, C., Osuna, D., Palacios-Rojas, N., Schindelasch, D., Thimm, O., Udvardi, M. K., and Stitt, M. (2004). Genome-wide reprogramming of primary and secondary metabolism, protein synthesis, cellular growth processes, and the regulatory infrastructure of Arabidopsis in response to nitrogen. Plant Physiol. **136:** 2483–2499.

Schmid, M., Davison, T.S., Henz, S.R., Pape, U.J., Demar, M., Vingron, M., Scholkopf, B., Weigel, D., and Lohmann, J.U. (2005). A gene expression map of *Arabidopsis thaliana* development. Nat. Genet. **37:** 501–506.

Semiarti, E., Ueno, Y., Tsukaya, H., Iwakawa, H., Machida, C., and Machida, Y. (2001). The ASYMMETRIC LEAVES2 gene of *Arabidopsis thaliana* regulates formation of a symmetric lamina, establishment of venation and repression of meristem-related homeobox genes in leaves. Development **128:** 1771–1783.

Shuai, B., Reynaga-Pena, C.G., and Springer, P.S. (2002). The lateral organ boundaries gene defines a novel, plant-specific gene family. Plant Physiol. **129:** 747–761.

Smyth, G.K. (2004). Linear models and empirical Bayes methods for assessing differential expression in microarray experiments. Stat. Appl. Genet. Mol. Biol. **3:** Article 3.

Solfanelli, C., Poggi, A., Loreti, E., Alpi, A., and Perata, P. (2006). Sucrose-specific induction of the anthocyanin biosynthetic pathway in Arabidopsis. Plant Physiol. **140:** 637–646.

Soyano, T., Thitamadee, S., Machida, Y., and Chua, N.H. (2008). ASYMMETRIC LEAVES2-LIKE19/LATERAL ORGAN BOUNDARIES DOMAIN30 and ASL20/LBD18 regulate tracheary element differentiation in *Arabidopsis*. Plant Cell **20:** 3359–3373.

Stitt, M. (1999). Nitrate regulation of metabolism and growth. Curr. Opin. Plant Biol. **2:** 178–186.

Stracke, R., Ishihara, H., Huep, G., Barsch, A., Mehrtens, F., Niehaus, K., and Weisshaar, B. (2007). Differential regulation of closely related R2R3-MYB transcription factors controls flavonol accumulation in different parts of the *Arabidopsis thaliana* seedling. Plant J. **50:** 660–677.

Takei, K., Takahashi, T., Sugiyama, T., Yamaya, T., and Sakakibara, H. (2002). Multiple routes communicating nitrogen availability from roots to shoots: A signal transduction pathway mediated by cytokinin. J. Exp. Bot. **53:** 971–977.

Taramino, G., Sauer, M., Stauffer, J.L., Jr., Multani, D., Niu, X., Sakai, H., and Hochholdinger, F. (2007). The maize (*Zea mays* L.) RTCS gene encodes a LOB domain protein that is a key regulator of embryonic seminal and post-embryonic shoot-borne root initiation. Plant J. **50:** 649–659.

Taylor, N.G., Howells, R.M., Huttly, A.K., Vickers, K., and Turner, S. R. (2003). Interactions among three distinct CesA proteins essential for cellulose synthesis. Proc. Natl. Acad. Sci. USA **100:** 1450–1455.

Teng, S., Keurentjes, J., Bentsink, L., Koornneef, M., and Smeekens, S. (2005). Sucrose-specific induction of anthocyanin biosynthesis in Arabidopsis requires the MYB75/PAP1 gene. Plant Physiol. **139:** 1840–1852.

Tohge, T., et al. (2005). Functional genomics by integrated analysis of metabolome and transcriptome of Arabidopsis plants over-expressing an MYB transcription factor. Plant J. **42:** 218–235.

Tschoep, H., Gibon, Y., Carillo, P., Armengaud, P., Szecowka, M., Nunes-Nesi, A., Fernie, A.R., Koehl, K., and Stitt, M. (2009). Adjustment of growth and central metabolism to a mild but sustained nitrogen-limitation in Arabidopsis. Plant Cell Environ. **32:** 300–318.

Tsukaya, H., Ohshima, T., Naito, S., Chino, M., and Komeda, Y. (1991). Sugar-dependent expression of the CHS-A gene for chalcone synthase from petunia in transgenic Arabidopsis. Plant Physiol. **97:** 1414–1421.

Udvardi, M.K., Czechowski, T., and Scheible, W.-R. (2008). Eleven golden rules of quantitative RT-PCR. Plant Cell **20:** 1736–1737.

Umehara, M., Hanada, A., Yoshida, S., Akiyama, K., Arite, T., Takeda-Kamiya, N., Magome, H., Kamiya, Y., Shirasu, K., Yoneyama, K., Kyozuka, J., and Yamaguchi, S. (2008). Inhibition of shoot branching by new terpenoid plant hormones. Nature **455:** 195–200.

Walch-Liu, P., Neumann, G., Bangerth, F., and Engels, C. (2000). Rapid effects of nitrogen form on leaf morphogenesis in tobacco. J. Exp. Bot. **51:** 227–237.

Wang, R., Okamoto, M., Xing, X., and Crawford, N.M. (2003). Microarray analysis of the nitrate response in Arabidopsis roots and shoots reveals over 1,000 rapidly responding genes and new linkages to glucose, trehalose-6-phosphate, iron, and sulfate metabolism. Plant Physiol. **132:** 556–567.

Wang, R., Tischner, R., Gutierrez, R.A., Hoffman, M., Xing, X., Chen, M., Coruzzi, G., and Crawford, N.M. (2004). Genomic analysis of the nitrate response using a nitrate reductase-null mutant of Arabidopsis. Plant Physiol. **136:** 2512–2522.

Wang, R., Xing, X., and Crawford, N.M. (2007). Nitrite acts as a transcriptome signal at micromolar concentrations in Arabidopsis roots. Plant Physiol. **145:** 1735–1745.

Wang, R., Xing, X., Wang, Y., Tran, A., and Crawford, N.M. (2009). A

genetic screen for nitrate-regulatory mutants captures the nitrate transporter gene NRT1.1. Plant Physiol. **135:** 472–478.

Wangwattana, B., Koyama, Y., Nishiyama, Y., Kitayama, M., Yamazaki, M., and Saito, K. (2008). Characterization of PAP1-upregulated glutathione S-transferase genes in *Arabidopsis thaliana*. Plant Biotechnol. **25:** 191–196.

Winkel-Shirley, B. (2001). It takes a garden. How work on diverse plant species has contributed to an understanding of flavonoid metabolism. Plant Physiol. **127:** 1399–1404.

Zhang, H., and Forde, B.G. (1998). An Arabidopsis MADS box gene that controls nutrient-induced changes in root architecture. Science **279:** 407–409.

Zhang, H., Jennings, A., Barlow, P.W., and Forde, B.G. (1999). Dual pathways for regulation of root branching by nitrate. Proc. Natl. Acad. Sci. USA **96:** 6529–6534.

Zimmermann, I.M., Heim, M.A., Weisshaar, B., and Uhrig, J.F. (2004). Comprehensive identification of *Arabidopsis thaliana* MYB transcription factors interacting with R/B-like BHLH proteins. Plant J. **40:** 22–34.